A NEW APPROACH TO DEFINE INTERNAL

PARTIAL DISCHARGE INTENSITY

by

Jerzy Wojciech Bania

A thesis

presented to the University of Manitoba

in partial fulfillment of the

requirements for the degree of

Doctor of Philosophy

in

Electrical Engineering

Winnipeg, Manitoba

THE UNIVERSITY OF MANITOBA

FACULTY OF GRADUATE STUDIES

The undersigned certify that they have read, and recommend to
the Faculty of Graduate Studies for acceptance, a Ph.D. thesis
entitled: ....
.......A NEW APPROACH TO DEFINE INTERNAL PARTIAL DISCHARGE ....
.......INTENSITY

....

submitted by ....JERZY W. BANIA.............................
in partial fulfilment of the requirements for the Ph.D. degree.

....
Advisor

....
....

Date of oral examination: ....December 12, 1985..........
The student has satisfactorily completed and passed the Ph.D.
oral examination.

....
Advisor

..Dr. S. Grzybowski....
External Examiner
..Docent, Technical Univ. of Poznan
..Poland.........

....
Chairman of Ph.D. Oral*

(*The signature of the Chairman does not necessarily signify that
the Chairman has read the complete thesis.)

A NEW APPROACH TO DEFINE INTERNAL

PARTIAL DISCHARGE INTENSITY

BY

JERZY WOJCIECH BANIA

A thesis submitted to the Faculty of Graduate Studies of
the University of Manitoba in partial fulfillment of the requirements
of the degree of

DOCTOR OF PHILOSOPHY

© 1985

To my family

I hereby declare that I am the sole author of this thesis.

I authorize the University of Manitoba to lend this thesis to other institutions or individuals for the purpose of scholarly research.

Jerzy Wojciech Bania

I further authorize the University of Manitoba to reproduce this thesis by photocopying or by other means, in total or in part, at the request of other institutions or individuals for the purpose of scholarly research.

Jerzy Wojciech Bania

The University of Manitoba requires the signatures of all persons using or photocopying this thesis. Please sign below, and give address and date.

_____

_____

_____

_____

_____

_____

_____

_____

_____

_____

_____

_____

_____

_____

_____

ABSTRACT

The results of measurements of internal partial discharge intensity generally are used to assess the risk of failure of electrical insulation due to internal discharges. However, with the use of present definitions of discharge intensity, there is as yet inadequate information for specifying acceptable levels of intensity.

The effectiveness of indicators of discharge intensity has been checked while maintaining "similar conditions" at all discharging cavities belonging to a set of insulation arrangements. Each arrangement consists of solid insulation with one air-filled cavity. A new, non-measurable quantity, the average discharge current transferred across the discharging cavity, has been introduced and its value is used to check if "similar conditions" exist in the cavity. Furthermore, a new and more accurate pattern of recurrence of discharges has been used to identify four groups of discharges, which in turn leads to a new definition of discharge intensity.

The results of computations of theoretical values of the new and presently used indicators are presented. Theoretical values of two most commonly used indicators are compared with published experimental results. The advantages associated with the use of the new definition are explained.

The results of computations indicate that, as an indicator, the new proposed definition of discharge intensity is relatively free from disadvantages associated with presently existing indicators.

ACKNOWLEDGEMENTS

The author wishes to express his gratitude to Professor
M. R. Raghuveer, for his invaluable guidance, support and encouragement.

Thanks are also due to Dean of Engineering E. Kuffel, for his support and encouragement.

CONTENTS

CONTENTS (continued)

LIST OF SYMBOLS

V_i — inception voltage for the cavity

ϵ_r — relative permittivity of solid insulation

ϵ_s — stress concentration factor

I_c — average discharge current transferred across the discharging cavity

V_{bd} — breakdown voltage of air

p — pressure

t — cavity depth or thickness of the layer

B — constant used to calculate V_{bd}

K — function of pt used to calculate V_{bd}

d — diameter of the cavity

C_c — capacitance of the cavity

C_b — capacitance of the dielectric in series with C_c

C_a — capacitance of the rest of the dielectric

V_a — voltage across the dielectric

V — voltage across the cavity

$*$ — superscript indicating commonly used pattern

V_c — fictitious voltage across the cavity in the absence of discharges

V_e — extinction voltage for the cavity

ΔV_c — voltage drop across the cavity due to a discharge

$+$ — superscript indicating positive polarity of the applied voltage

$-$ — superscript indicating negative polarity of the applied voltage

k — discharge coefficient related to V_i and ΔV_c

i   -   number of discharges per cycle

m   -   number of discharges per quarter-cycle

^   -   superscript indicating the peak value

ΔV_a -   voltage drop across the dielectric due to a discharge

ΔV_b -   voltage gain across the dielectric in series with the cavity due to a discharge

V_b -   voltage across capacitance C_b

ΔV_{cr} -   voltage gain across the cavity due to recharging

ΔV_{br} -   voltage gain across the dielectric in series with the cavity due to recharging

ΔV_{ar} -   voltage gain across the dielectric due to recharging

E_c -   energy stored in capacitance C_c

E_b -   energy stored in capacitance C_b

E_a -   energy stored in capacitance C_a

'   -   superscript indicating the energy state (i) before the occurrence of a discharge

''   -   superscript indicating the energy state (ii) after the occurrence of a discharge

'''   -   superscript indicating the energy state (iii) after recharging

ΔV_{ct} -   effective voltage drop across the cavity due to a discharge and subsequent recharging

V_r -   voltage across the cavity after recharging

ΔV_{bt} -   effective voltage gain across the dielectric in series with the cavity due to a discharge and subsequent recharging

q   -   apparent charge

q_c -   amount of charge actually transferred across the cavity

n   -   repetition rate

w   -   energy of an individual discharge

U_i — inception voltage for the insulation

I — average discharge current

T — time interval or cycle of the applied voltage

D — quadratic rate

P — discharge power

U_k — instantaneous value of V_a at the instant of kth discharge

U_e — extinction voltage for the insulation

un — subscript indicating group of unlike discharges in negative half-cycle

lp — subscript indicating group of like discharges in positive half-cycle

up — subscript indicating group of unlike discharges in positive half-cycle

ln — subscript indicating group of like discharges in negative half-cycle

h — diameter of the electrodes

l — number of layers of the solid dielectric

E_{av} — average electric stress between electrodes

ϵ_0 — the permittivity of vacuum

R — reference number used to calculate m

j — number of discharges per half-cycle

f — frequency of the applied voltage

V_{ck} — instantaneous value of V_c at the instant of kth discharge

n_u — repetition rate of unlike discharges

n_l — repetition rate of like discharges

ΔE_{diss} — energy dissipated due to a discharge

ΔE_{supp} — energy supplied due to recharging from the voltage source

ΔE — total energy change due to a discharge and subsequent recharging from the voltage source

LIST OF TABLES

LIST OF FIGURES

CHAPTER I

INTRODUCTION

1.1   BACKGROUND, MOTIVATION AND OBJECTIVE

A partial discharge is an electric discharge that partially bridges the insulation between conductors. These discharges may, or may not, occur adjacent to a conductor. The partial discharge that occurs in inclusions or cavities in a dielectric is called an internal partial discharge or just an internal discharge. Internal discharges in insulation occur commonly in gas-filled cavities. If these discharges occur in cavities in dielectrics, they cause progressive reduction of the electric strength with time. Internal discharges may cause progressive degradation of insulation by erosion or chemical degradation, and ultimate failure of insulation may be caused by tree propagation or cumulative heating [1]. Measurements of discharge intensity are made for assessing the relative resistance of materials to internal discharges.

It is of great practical importance to define precisely the term "internal partial discharge intensity". Measurements of discharge intensity are carried out to assess the risk of failure of electrical insulation by the action of internal discharges. However, there is as yet inadequate information for specifying acceptable levels of discharge intensity for many types of insulation and service conditions [1]. Therefore, the introduction of a new definition of discharge intensity may lead to a better interpretation of the results of measurements.

The objective of this thesis is to propose a new definition of

internal partial discharge intensity which, as an indicator, will be relatively free from disadvantages associated with presently existing indicators. The new definition is comprised of the values of two of the new indicators of discharge intensity proposed in this work.

1.2   MAJOR PROCEDURES EMPLOYED IN THE THESIS

The internal discharges analyzed in this thesis occur under the application of alternating voltage to solid insulation arrangements, each arrangement consisting of one air-filled cavity. The cavities are disc shaped with the diameter of the disc exceeding its thickness. The field in the cavity is uniform.

Such a choice is justified from three points of view. First, it is important to carry out such studies under uniform field conditions. Secondly, it allows the calculation of the inception voltage of discharges, V_i, with good accuracy. Lastly, the electric stress concentration factor, ϵ_s, for such types of cavities is equal to ϵ_r, the relative permittivity of the solid insulation, and is higher than the factor which is obtained with either a spherical cavity or a disc shaped cavity whose thickness exceeds its diameter.

In order to check the effectiveness of an indicator of partial discharge intensity, "similar conditions" are maintained at all the discharging cavities belonging to a set of insulation arrangements. To facilitate this, a new, nonmeasurable quantity, I_c, has been introduced. I_c is the average discharge current transferred across the discharging cavity and its value may be used to check if "similar conditions" do exist.

Also, a new and more accurate pattern of recurrence of discharges, introduced in earlier work [2], has been used. From this recurrence pattern, four groups of discharges have been identified. Such a grouping leads to a new definition of discharge intensity.

Theoretical values of the new and presently used indicators have been computed for a series of insulation arrangements representing laboratory model insulation. Theoretical values of two most commonly used indicators have been compared with published experimental results. The advantages associated with the use of the new definition of discharge intensity have been explained.

1.3   OUTLINE OF THE THESIS

The importance of studies of internal partial discharge intensity, the objective of this thesis, and the procedures employed to achieve the objective, are briefly explained in this chapter.

In Chapter II the phenomena associated with internal partial discharges are discussed.

Chapter III presents the analysis of recurrence of discharges, which results in the grouping of discharges.

In Chapter IV the presently used definitions of discharge intensity are presented, new quantities are proposed and a new definition of discharge intensity is introduced.

Chapter V covers the procedures of computations of theoretical values of the new and presently used indicators of discharge intensity.

Chapter VI presents the evaluation of the new and presently used indicators of discharge intensity, carried out for a set of insulation arrangements.

In Chapter V.II the results of computations are compared with recently published experimental results.

The advantages associated with use of the new definition of discharge intensity are explained in Chapter VIII.

Final conclusions, major contributions and suggestions for further research are stated in Chapter IX.

CHAPTER II

INTERNAL PARTIAL DISCHARGES

2.1   INTRODUCTION

In this chapter the phenomena associated with internal discharges are discussed.

Different methods of computing the breakdown voltage of air in a cavity are reviewed.   The commonly used equivalent circuit of a dielectric is described and the commonly used pattern of recurrence of discharges is explained.

2.2   BREAKDOWN STRENGTH OF GAS-FILLED CAVITY

The dielectric properties of inclusions or cavities in insulation are usually inferior to those of the insulation [3].   If the voltage applied to insulation just exceeds the voltage necessary to initiate discharges in inclusions or cavities in insulation, discharges will occur after a certain time lag [3].   Internal discharges may occur upon application of alternating voltage, direct voltage and also single impulses [1].   In this thesis, internal discharges occurring, due to application of alternating voltage, in gas (namely air) filled cavities in solid insulation, will be considered.

The electric stress in a gas-filled cavity depends on its shape and dimensions, on the relative permittivity ϵ_r of the surrounding insulation and on the inhomogeneity of the electric field.   The dielectric strength of a gas-filled cavity depends on the type of gas in it, its pressure, and the cavity dimensions.   The discharges occur between the

cavity walls at about the same voltage as would be required between equally spaced metal electrodes [3,4]. The discharge inception voltage may therefore be found by application of Paschen's Law [4]. The voltage necessary to initiate discharges can be predicted to about ±15% when alternating voltage is applied to discs containing a cylindrical flat cavity perpendicular to the field [1]. In this case the cavity is stressed at ϵ_r times the stress in the surrounding dielectric. However, the actual breakdown strength of the cavity may vary considerably from that predicted, due to the effect of semiconducting layers on the cavity walls and static charges, either produced when the cavity was formed or left from previous discharges.

The breakdown strength of air as a function of pressure and electrode spacing is shown in Fig. 2.1 [5].

The breakdown voltage, V_{bd}, of air as a function of pressure p and electrode spacing t can also be calculated for a wide range of pt values using formula (2.1) from recent literature [6]; the computed values of V_{bd} are accurate to about ±3% of the measured values

$$V_{bd} = \frac{Bpt}{\ln(pt) + K} \tag{2.1}$$

where: B = 2737.5 V/kPa-cm,

K is a function of pt as shown in Table 2.1.

Fig. 2.2, [6], compares the "Paschen curves," for different gases, obtained experimentally and by application of formula (2.1).

In earlier works [7,8] a linear approximation was used to compute the values of the breakdown voltage, V_{bd}, of air in the cavity, as a
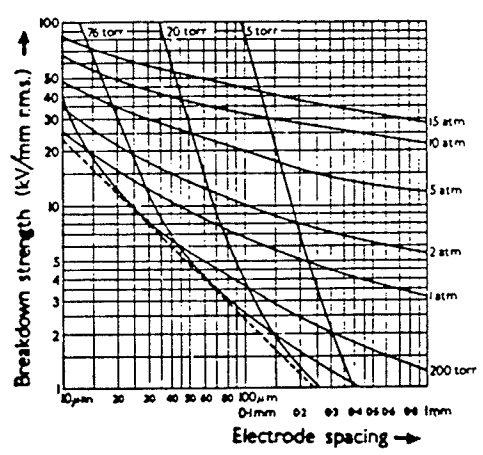
Fig. 2.1: The breakdown strength of air in kV/mm r.m.s. as a function of pressure and distance between opposite electrodes (derived from "Paschen curve") [5].
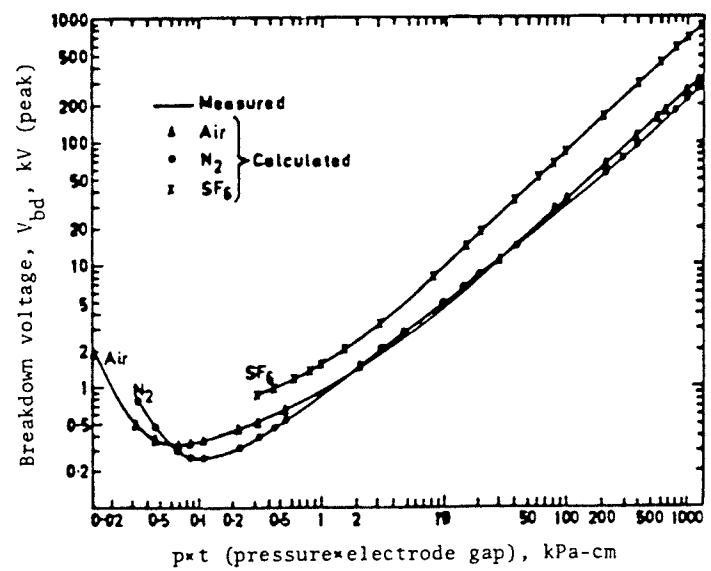
Fig. 2.2: Measured and calculated "Paschen curves" for air, N_2 and SF_6 [6].

Table 2.1

K for Air as a Function of pt [6]

pt [kPa-cm]	K [-]
0.0133 - 0.2	$2.0583 \, (pt)^{-0.1724}$
0.2 - 100	$3.5134 \, (pt)^{0.0599}$

Table 2.2

Approximation of V_{bd} of Air as a Function of t at 1 atm

t [mm]	$V_{bd} = f(t)$ [V (peak)]
0.01 - 0.1	$333 + 6670 \, t$
0.1 - 1	$620 + 3880 \, t$
1 - 10	$1600 + 2840 \, t$

function of the cavity depth t at a pressure of 1 atm. This approximation is shown in Table 2.2.

The breakdown strength of air in a spherical cavity has been reported in [5] and the results were used in partial discharge tests to determine the applied voltage [9]. This breakdown strength is shown in Fig. 2.3.

The electric stresses in elliptic cylindrical and oblate spheroidal gas-filled cavities were considered in [10] and the formulae, relating electric stress in the cavity to applied voltage and geometry of the cavity, were obtained neglecting the effects of volume and surface conductivities of the cavities. If either of these conductivities is appreciable the electric stress in the cavity may be significantly reduced.

The effect of geometry and orientation of cavity on the stress concentration factor, ϵ_s, for cavities of simple geometrical shapes is shown in Fig. 2.4 [1].

2.3   EQUIVALENT CIRCUIT

The behaviour of internal discharges with alternating voltage can be described conveniently with the aid of the commonly used equivalent circuit shown in Fig. 2.5 [1,2,3,5,7,8,11,12,13,14,15]. The capacitance of the cavity is represented by C_c, the capacitance of the dielectric in series with C_c is represented by C_b, and the capacitance of the rest of the dielectric is represented by C_a.

2.4   COMMONLY USED PATTERN OF RECURRENCE OF DISCHARGES

Fig. 2.6 [5] shows the high voltage V_a^* across the dielectric, the
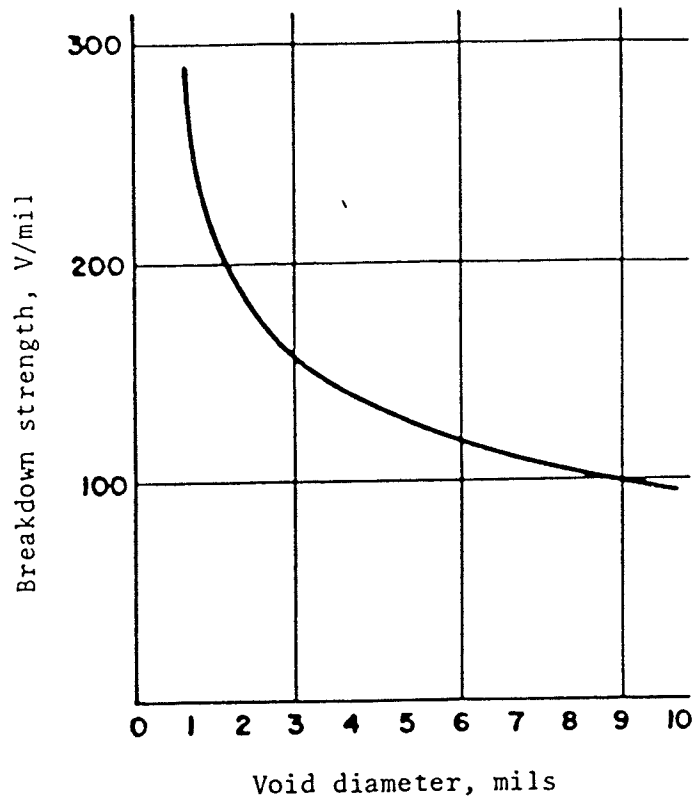
Fig. 2.3: Calculated breakdown strength of air in a spherical cavity versus diameter at 1 atm [5].
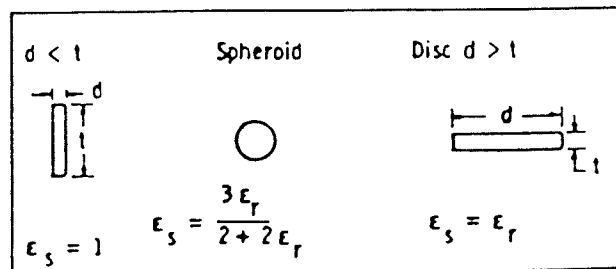
Fig. 2.4: Effect of geometry and orientation of cavity on the stress concentration factor ϵ_s [1].
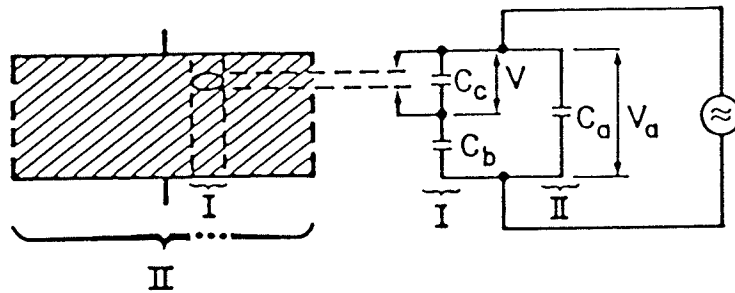
Fig. 2.5: Representation of a cavity in the dielectric:
I   corresponds to faulty part of the dielectric;
II   corresponds to healthy part of the dielectric.
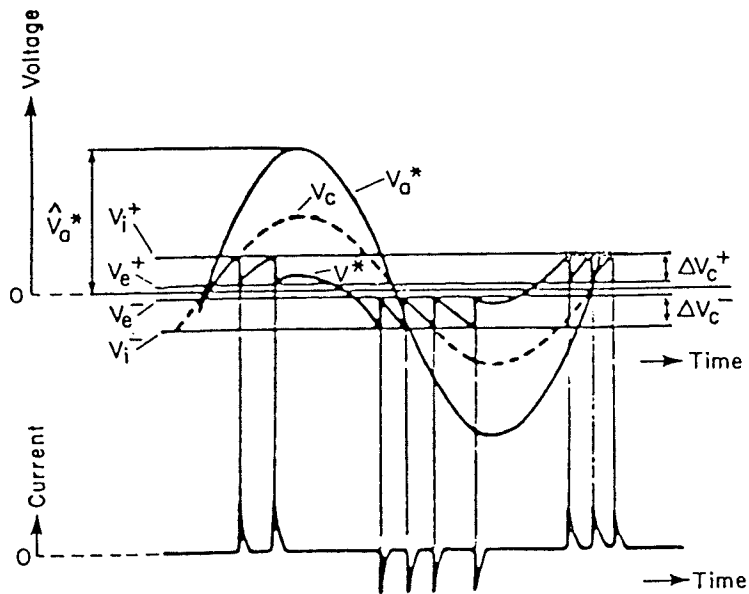
Fig. 2.6: Recurrence of internal discharges [5].

voltage V* across the cavity, the fictitious voltage V_c across the cavity in the absence of discharges, and the current impulses associated with individual discharges; the usefulness of these impulses is demonstrated in Section 3.4.

When the voltage V* reaches the discharge inception voltage for the cavity, V_i^+, a discharge occurs in the cavity; V_i^+ may be found from the "Paschen curve." Then, the voltage V* drops to the discharge extinction voltage for the cavity, V_e^+, when the discharge extinguishes. This voltage drop takes place in less than 10^{-7} s; compared with the duration of a 60 Hz sine wave the voltage drop may be regarded as a step function [5]. After discharge extinction, the voltage V* across the cavity rises to V_i^+ again when the next discharge occurs. This happens several times, after which the applied voltage V_a^* decreases and the voltage V* decreases until it reaches V_i^- when a new discharge occurs. In this way a series of regularly recurrent discharges will be found. The voltage V* across the cavity is determined by the superposition of the external electric field and the field of the surface charges on the cavity walls due to the last discharge. It is often assumed [5] that the voltages V_i and V_e and the voltage drop ΔV_c are polarity independent, namely: V_i^+ = V_i^-, V_e^+ = V_e^-, and ΔV_c^+ = ΔV_c^-. The above relations are also assumed in this thesis.

The voltage drop ΔV_c which occurs across the cavity because of appearance of internal discharge is expressed by

$$\Delta V_c = V_i - V_e \qquad (2.2)$$

where: V_i is the internal discharge inception voltage between opposite walls of the cavity,

V_e is the discharge extinction voltage across the cavity.

As in [7,8] it is assumed that

$$\Delta V_c = k V_i \tag{2.3}$$

where k is a discharge coefficient, $0 < k < 1$.

It follows from (2.2) and (2.3) that the voltage V_e is equal to

$$V_e = (1-k) V_i \tag{2.4}$$

It may be obtained, as in [2], from Fig. 2.6 that the number i of internal discharges per cycle of alternating voltage is

$$i = 4m^\star \tag{2.5}$$

where $m^\star$ is the largest integer which satisfies

$$m^\star \leq \frac{\hat{V}_c - V_e}{V_i - V_e} = \frac{\hat{V}_c - V_e}{\Delta V_c} \tag{2.6}$$

and $\hat{V}_c$ is the peak value of V_c.

On the basis of the equivalent circuit of Fig. 2.5 the peak value of the voltage V_c is equal to [13]

$$\hat{V}_c = \frac{C_b}{C_c + C_b} \hat{V}_a \tag{2.7}$$

where $\hat{V}_a$ is the peak value of V_a.

An individual internal discharge causes the voltage drops ΔV_c across the cavity and ΔV_a across the dielectric between the electrodes; it is also responsible for the voltage gain ΔV_b across the dielectric in series with the cavity. On the basis of the equivalent circuit of Fig. 2.5, ΔV_a and ΔV_b are expressed as the following functions of ΔV_c [13]

$$\Delta V_a = \frac{C_b}{C_b + C_a} \Delta V_c \tag{2.8}$$

and

$$\Delta V_b = \frac{C_a}{C_b + C_a} \Delta V_c \tag{2.9}$$

2.5   SUMMARY

The available methods from literature of computing the breakdown voltage of air in a cavity have been presented.   The method to be employed in computations will be chosen in Chapter V.

The commonly used equivalent circuit of a dielectric, which will be used throughout this thesis, has been described and the associated commonly used pattern of recurrence of discharges explained.   This pattern will be critically examined in the next chapter.

CHAPTER III

ANALYSIS OF RECURRENCE OF DISCHARGES

3.1   INTRODUCTION

In this chapter a critical analysis of the commonly used pattern of recurrence of discharges is carried out. Based on three characteristic energy states, a new and more accurate pattern of recurrence of discharges, introduced in earlier work [2], is explained.

This pattern of recurrence is used to identify four groups of discharges.

3.2   THREE CHARACTERISTIC ENERGY STATES

The equivalent circuit shown in Fig. 2.5 is commonly used in the literature [1,3,5,7,8,11,12,13,14,15] together with the pattern of recurrence of internal discharges shown in Fig. 2.6. The formulae (2.5), (2.6) and (2.7) correctly describe the process of a discharge. However, as shown in earlier work [2], use of these formulae in combination with the pattern of recurrence of internal discharges, Fig. 2.6, leads to the conclusion that the energy balance of the discharges is not satisfied. The energy balance was calculated by comparing the energy dissipated due to the discharges with the energy supplied from the voltage source, for one cycle of alternating voltage.

In earlier work [2], three characteristic energy states were proposed. The assumption was made that the time intervals between these states for an individual discharge are negligibly short when the applied voltage has a frequency of either 50 Hz or 60 Hz; the voltage drops or

gains between these states may therefore be regarded as step functions. It was shown in [2] that this assumption does not affect the energy balance of the discharges.

The energy states are [2]:

(i)   state (just) before the occurrence of a discharge,

(ii)   state (just) after the occurrence of a discharge,

(iii) state (just) after recharging of the insulation from the voltage source.

These energy states are illustrated in Fig. 3.1 and the associated quantities are shown in Table 3.1 [2].

After the discharge extinction the voltage source compensates for the voltage drop ΔV_a, across the dielectric, which is caused by the discharge, and the voltage gain across the dielectric due to its recharging, ΔV_{ar}, is equal to ΔV_a. This equality is used in Table 3.1. The recharging of the insulation from the voltage source also produces the voltage gains ΔV_{cr} across the cavity and ΔV_{br} across the dielectric in series with the cavity [2]. On the basis of the equivalent circuit of Fig. 2.5, ΔV_{cr} and ΔV_{br} can be expressed as follows [2]

$$\Delta V_{cr} = \frac{C_b}{C_c + C_b} \Delta V_{ar}$$

$$= \frac{C_b}{C_c + C_b} \Delta V_a \qquad (3.1)$$

and

$$\Delta V_{br} = \frac{C_c}{C_c + C_b} \Delta V_{ar}$$

$$= \frac{C_c}{C_c + C_b} \Delta V_a \qquad (3.2)$$
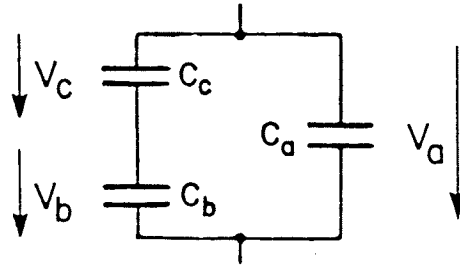
a)   state (i)

b)   state (ii)
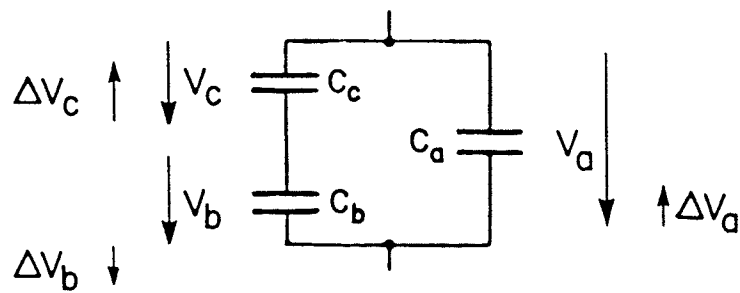
c)   state (iii)
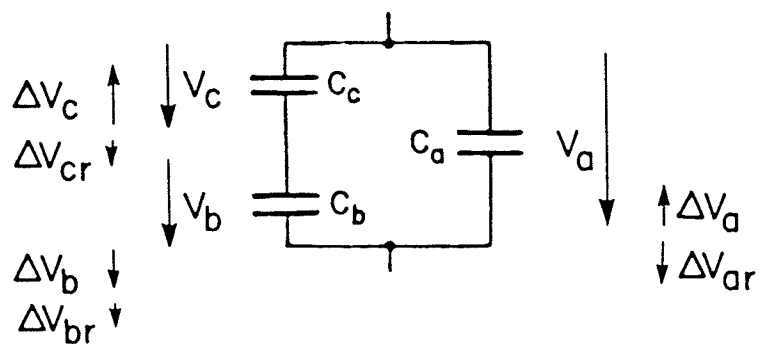
Fig. 3.1: Illustration of three energy states: a) (just) before the occurrence of a discharge, b) (just) after the occurrence of a discharge, and c) (just) after recharging of the insulation from the voltage source.

Table 3.1

Capacitance, Voltage and Energy for Three Energy States [2]

Energy State	Capacitance	Voltage	Energy
(i) Before the Occurrence of a Discharge	C_c	$V_c = V_i$	$E_c' = \frac{1}{2} C_c V_i^2$
	C_b	$V_b = V_a - V_i$	$E_b' = \frac{1}{2} C_b (V_a - V_i)^2$
	C_a	V_a	$E_a' = \frac{1}{2} C_a V_a^2$
(ii) After the Occurrence of a Discharge	C_c	$V_c - \Delta V_c = V_e = V_i - \Delta V_c$	$E_c'' = \frac{1}{2} C_c (V_i - \Delta V_c)^2$
	C_b	$V_b + \Delta V_b = V_a - V_i + \Delta V_b$	$E_b'' = \frac{1}{2} C_b (V_a - V_i + \Delta V_b)^2$
	C_a	$V_a - \Delta V_a$	$E_a'' = \frac{1}{2} C_a (V_a - \Delta V_a)^2$
(iii) After Recharging	C_c	$V_c - \Delta V_c + \Delta V_{cr} = V_i - \Delta V_c + \Delta V_{cr}$	$E_c''' = \frac{1}{2} C_c (V_i - \Delta V_c + \Delta V_{cr})^2$
	C_b	$V_b + \Delta V_b + \Delta V_{br} = V_a - V_i + \Delta V_b + \Delta V_{br}$	$E_b''' = \frac{1}{2} C_b (V_a - V_i - \Delta V_b + \Delta V_{br})^2$
	C_a	$V_a - \Delta V_a + \Delta V_{ar} = V_a$	$E_a''' = \frac{1}{2} C_a V_a^2$

The effective voltage drop ΔV_{ct} across the cavity, due to a discharge and subsequent recharging can be expressed by

$$\Delta V_{ct} = \Delta V_c - \Delta V_{cr}$$
$$= V_i - \dot{V}_r \tag{3.3}$$

where V_r is the voltage across the cavity after the recharging.

3.3   NEW PATTERN OF RECURRENCE OF DISCHARGES

The three characteristic energy states illustrated in Fig. 3.1 lead to the new and more accurate pattern of recurrence of internal discharges introduced in [2]. This pattern is shown in Fig. 3.2 and identified by the symbol V. Using this pattern of recurrence of internal discharges it was proved [2] that the energy balance of discharges, calculated for one cycle of alternating voltage, is satisfied. For comparison, the pattern commonly used in literature has been shown in Fig. 3.2 and identified by the symbol V*. As can be seen from Fig. 3.2, these two patterns yield different numbers of discharges per cycle of alternating voltage; the instants at which the discharges occur are also different. It may be noticed that the difference between the two patterns diminishes as the inequalities $C_a \gg C_b$ and $C_c \gg C_b$ get more pronounced. The above inequalities are true for most practical insulation systems but may not be true for many laboratory model insulation systems.

It may be obtained, [2], from the new pattern of recurrence, shown in Fig. 3.2, that the number i of internal discharges per cycle of alternating voltage is

$$i = 4m \tag{3.4}$$
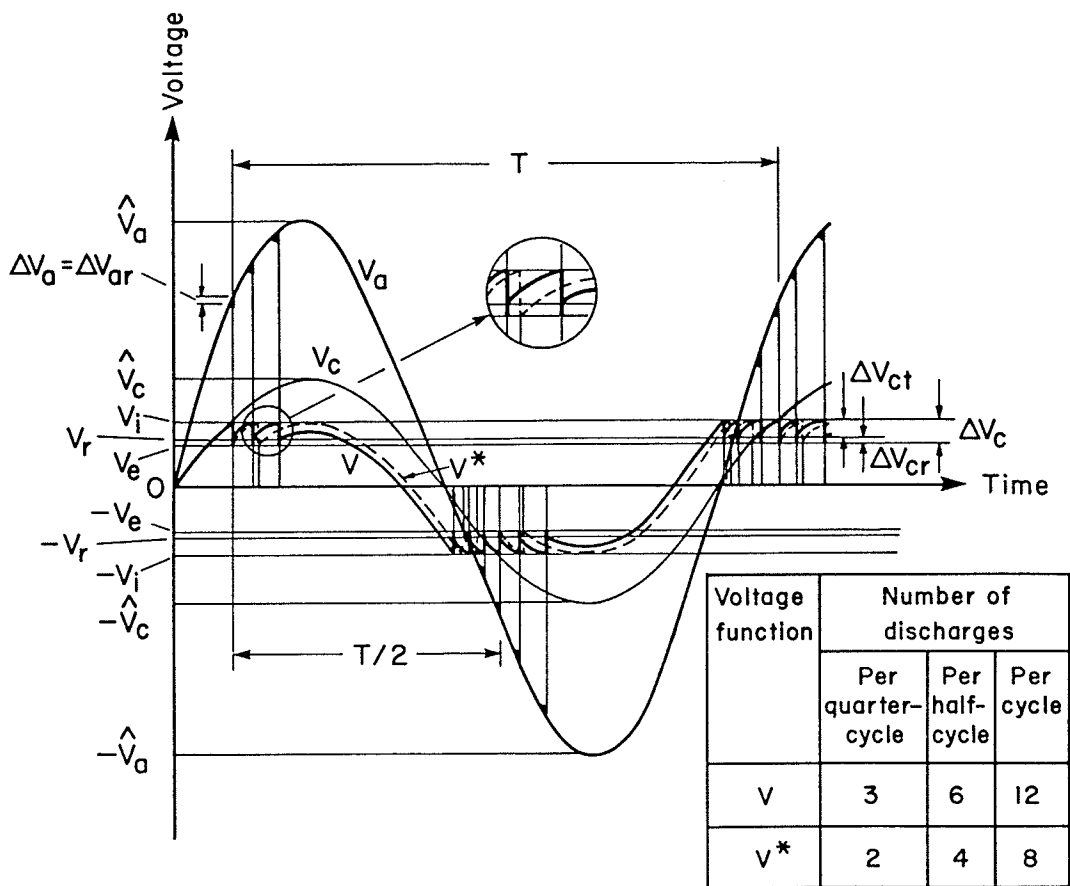
Fig. 3.2: Two different patterns of recurrence of internal discharges:
    voltage function V - new pattern;
    voltage function V* - commonly used pattern.

where m is the largest integer which satisfies

$$m \leq \frac{\hat{V}_c - V_r}{V_i - V_r} = \frac{\hat{V}_c - V_r}{\Delta V_{ct}} \tag{3.5}$$

It may be noticed that the expression on the right hand side of the inequality (3.5), obtained for the new pattern of recurrence, differs from the expression on the right hand side of inequality (2.6), obtained for the commonly used pattern of recurrence. Therefore these different patterns, in general, yield different numbers of discharges per cycle.

The new pattern is considered to be more accurate because it does not violate the energy balance of the discharges i.e. energy dissipated per cycle due to discharges is equal to energy supplied per cycle by the source. The differences in the two patterns of recurrence are due to the inclusion, in the new pattern, of the process of recharging of the insulation from the voltage source. The voltage gains produced by recharging are ΔV_{ar} across the dielectric, ΔV_{cr} across the cavity and ΔV_{br} across the dielectric in series with the cavity. The voltage gains ΔV_{ar} and ΔV_{cr} are identified in Fig. 3.2.

The differences between the two patterns of recurrence are even more evident in Fig. A.1 (in the Appendix) due to the smaller number of discharges per cycle. This makes it easier to show, in Fig. A.1, not only two different functions of voltage across the cavity: V - for the new pattern and V* - for the commonly used pattern, but also the different functions of voltage across the dielectric: V_a - for the new pattern and V_a* - for the commonly used pattern. The latter two functions differ only during the time of occurrence of a discharge and subsequent recharging; otherwise they are identical. Because of this reason and

also due to the fact that the number of discharges per cycle in Fig. 3.2 is larger, the function V_a^* has not been shown in that Figure. The case of discharges shown in Fig. A.1 has been used in the Appendix to conduct a typical energy balance in order to illustrate the effect of neglecting, in the commonly used pattern of recurrence, insulation recharging by the voltage source.

3.4   PROPOSED GROUPS OF DISCHARGES

As can be seen from Fig. 2.6 an individual internal discharge is accompanied by either a positive or a negative current impulse which is a measurable quantity. The occurrence of these current impulses makes the electrical detection and measurements of internal partial discharges possible. In Fig. 3.2 all discharges of positive current impulses occur in the positive half-cycle of the voltage sine wave and all discharges of negative current impulses occur in the negative half-cycle of the voltage sine wave. This, however, is not always the case. It is therefore possible to identify four groups of discharges, which are shown in Fig. 3.3 where the new pattern of recurrence has been used.

The groups of discharges will be classified as follows.

(un) - group of discharges of positive impulses in negative half-
       cycle: unlike discharges in negative half-cycle;

(1p) - group of discharges of positive impulses in positive half-
       cycle: like discharges in positive half-cycle;

(up) - group of discharges of negative impulses in positive half-
       cycle: unlike discharges in positive half-cycle;

(1n) - group of discharges of negative impulses in negative half-
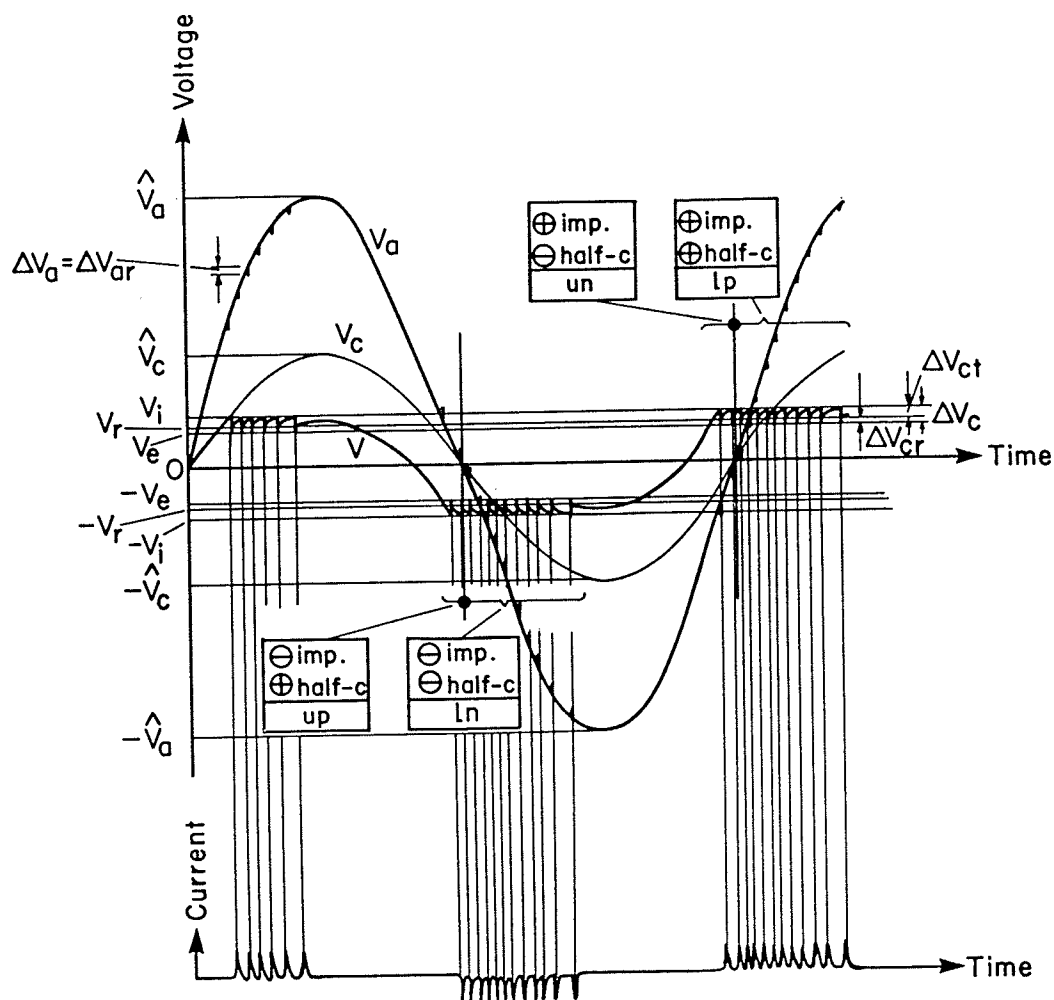
Fig. 3.3: Four groups of discharges:
  un - unlike discharges in negative half-cycle;
  lp - like discharges in positive half-cycle;
  up - unlike discharges in positive half-cycle;
  ln - like discharges in negative half-cycle.

cycle: like discharges in negative half-cycle.

Such a grouping of discharges is also possible if the commonly used pattern of recurrence is employed.

3.5   CONCLUSIONS

A critical analysis of the commonly used pattern of recurrence of discharges has been carried out, and, the new and more accurate pattern of recurrence of discharges, introduced in earlier work [2], explained. The new pattern is considered to be more accurate because, as opposed to the commonly used pattern, it does not violate the energy balance of discharges i.e. energy dissipated per cycle due to discharges is equal to energy supplied per cycle by the voltage source. A typical energy balance calculation is conducted in the Appendix in order to illustrate the effect of neglecting, in the commonly used pattern of recurrence, insulation recharging from the voltage source.

It has been noticed that the difference between the two patterns of recurrence diminishes as the inequalities $C_a \gg C_b$ and $C_c \gg C_b$ get more pronounced. The above inequalities are true for most practical insulation systems but may not be true for many laboratory model insulation systems.

The new pattern of recurrence has been used to identify four groups of discharges: (un) - unlike discharges in negative half-cycle, (lp) - like discharges in positive half-cycle, (up) - unlike discharges in positive half-cycle, and (ln) - like discharges in negative half-cycle. This grouping will lead to a new definition of discharge intensity which will be introduced in the next chapter.

CHAPTER IV

DEFINITIONS OF INDICATORS OF INTERNAL PARTIAL DISCHARGE INTENSITY

4.1   INTRODUCTION

In this chapter the presently used definitions of indicators of internal partial discharge intensity are reviewed.

A new, nonmeasurable quantity, the average discharge current transferred across the discharging cavity, is introduced. Moreover, based on the identification of four groups of discharges, new indicators of discharge intensity are proposed.

Next, a new definition of discharge intensity is introduced.

.

4.2   PRESENTLY USED INDICATORS

Partial discharge intensity is a general comparative term for the amount of partial discharge. There are several indicators of partial discharge intensity which are quantitative partial discharge parameters. Quantitative results of partial discharge measurements are expressed in terms of one or more of these indicators. Indicators of partial discharge intensity are specified quantities defined as follows [16].

<1> Quantities related to individual discharges

<1a> Apparent charge, q

The apparent charge q of a partial discharge is that charge which, if injected instantaneously between the terminals of the test object,

would momentarily change the voltage between its terminals by the same amount as the partial discharge itself. The absolute value $|q|$ of the apparent charge is often referred to as the discharge magnitude. The apparent charge is expressed in coulombs.

Note. - The apparent charge q so defined is not equal to the amount of charge, q_c, actually transferred across the discharging cavity in the dielectric. It is used because discharge measuring instruments respond to this quantity.

<1b> Repetition rate, n

The partial discharge pulse repetition rate n is the average number of partial discharge pulses per second.

Note. - In practice only pulses above a specified magnitude, or within a specified range of magnitudes, may be considered. The results are sometimes expressed as cumulative frequency distribution curves of partial discharge magnitudes.

<1c> Energy, w, of an individual discharge

The partial discharge energy w is the energy dissipated during one individual discharge; it is expressed in joules.

Note. - Under certain assumptions regarding the electrical representation of the physical phenomenon, this energy is given, in terms of q and U_i by

$$w = \sqrt{2} \cdot \frac{1}{2} q U_i \tag{4.1}$$

where: q is the measured apparent charge

U_i is the corresponding value of the inception voltage.

For definition of the inception voltage, see <3> and <3a>.

Note that U_i is given as peak value divided by $\sqrt{2}$.

<2> Integrated quantities

From the basic quantities, q and n, other quantities can be defined, which are characterized by summations over a time interval T. This time should be long compared with the duration of one cycle of the voltage supplied to the test object.

<2a> Average discharge current, I

The average discharge current, I, is the sum of the rectified charge quantities passing through the terminals of a test object due to partial discharges, during a certain time interval, T, divided by this time interval:

$$I = \frac{1}{T} \left[\left| q_i \right| + \left| q_2 \right| + \left| q_3 \right| + \ldots + \left| q_i \right| \right] \qquad (4.2)$$

If all discharges are of equal magnitude, $\left| q \right|$, this simplifies to

$$I = n \left| q \right| \qquad (4.3)$$

The average discharge current is expressed in coulomb/second (ampere).

<2b> Quadratic rate, D

The quadratic rate, D, is the sum of the squares of charges passing through the terminals of the test object due to partial discharges, during a certain time interval, T, divided by this time interval:

$$D = \frac{1}{T} [q_1^2 + q_2^2 + q_3^2 + \ldots + q_i^2] \qquad (4.4)$$

If all discharges are of equal magnitude, $|q|$, this simplifies to

$$D = nq^2 \qquad (4.5)$$

The quadratic rate is expressed in $(coulomb)^2/second$.

<2c> Discharge power, P

The discharge power, P, is the average power fed into the terminals of the test object due to partial discharges during a certain time interval, T.

This is given by

$$P = \frac{1}{T} [q_1 U_1 + q_2 U_2 + q_3 U_3 + \ldots + q_i U_i] \qquad (4.6)$$

where: U_1, U_2 ... U_i are the instantaneous values of the voltage across the test object at the instants of discharges q_1, q_2 ... q_i. The average discharge power is expressed in watts.

<3> Voltage values related to partial discharges

Voltage values during partial discharge tests are usually given by their peak values divided by $\sqrt{2}$. The following values are of particular interest.

<3a> Partial discharge inception voltage, U_i

The partial discharge inception voltage U_i is the lowest voltage at which partial discharges exceeding a specified intensity are observed, under specified conditions, when the voltage applied to the test object

is gradually increased from a lower value at which no such discharges are observed.

<3b> Partial discharge extinction voltage, U_e

The partial discharge extinction voltage U_e is the voltage at which partial discharges exceeding a specified intensity cease, under specified conditions, when the voltage is gradually decreased from a value exceeding the inception voltage.

<3c> Assured partial discharge free test voltage

The assured partial discharge free test voltage is a specified voltage applied in a specified test procedure at which the test object should be free from partial discharges exceeding a specified intensity.

The above nine specified quantities <1a>, <1b>, <1c>, <2a>, <2b>, <2c>, <3a>, <3b>, and <3c> are recommended by the International Electro-technical Commission [16]. Five of the above quantities, namely <1a>, <2a>, <3a>, <3b>, and <3c> are used in the recommended practice by the American National Standards Institute/Institute of Electrical and Electronics Engineers [17], and another two, namely <1c> and <2c> are defined for future reference but are not used in this recommended practice. Of the nine quantities recommended by IEC, six, namely <1a>, <1b>, <1c>, <2c>, <3a>, and <3b> are the same as, or similar to, the quantities specified by the American Society for Testing and Materials in the standard [18].

Indicators of partial discharge intensity referred to internal partial discharges may be called indicators of internal partial discharge intensity.

4.3   NEW NONMEASURABLE QUANTITY

It is convenient to introduce a new, nonmeasurable quantity. This is the average discharge current transferred across the discharging cavity in the dielectric, I_c. This current is defined in the following way; its usefulness is demonstrated in Chapter VI.

The average discharge current transferred across the discharging cavity in the dielectric, I_c, is the sum of the rectified charge quantities being transferred across the cavity during a certain time interval, T, divided by this time interval:

$$I_c = \frac{1}{T} \left[\left| q_{c1} \right| + \left| q_{c2} \right| + \left| q_{c3} \right| + \ldots + \left| q_{ci} \right| \right] \qquad (4.7)$$

If all discharges are of equal magnitude, $\left| q_c \right|$, this simplifies to

$$I_c = n \left| q_c \right| \qquad (4.8)$$

The average discharge current transferred across the discharging cavity in the dielectric is expressed in coulomb/second (ampere).

As mentioned earlier, I_c is used to ascertain whether similar conditions exist at the discharge sites in a set of insulation arrangements. If the values of I_c do not differ significantly, "similar conditions" prevail at the discharging cavities of a set.

4.4   PROPOSED NEW INDICATORS

It is proposed that the following indicators of internal partial discharge intensity, presented in Section 4.2, be considered separately for individual groups of discharges (un), (1p), (up) and (1n):

    <1a> apparent charge, q,

    <1b> repetition rate, n,

<2a> average discharge current, I,

<2b> quadratic rate, D,

<2c> discharge power, P.

New proposed indicators of internal partial discharge intensity are introduced in Table 4.1.

It may be noticed that n_{un}, n_{1p}, n_{up} and n_{1n} are the components of the repetition rate, n; I_{un}, I_{1p}, I_{up} and I_{1n} are the components of the average discharge current, I; D_{un}, D_{1p}, D_{up} and D_{1n} are the components of the quadratic rate, D; and finally that P_{un}, P_{1p}, P_{up} and P_{1n} are the components of the discharge power, P.

In addition, the nonmeasurable average discharge current trans-ferred across the discharging cavity in the dielectric, I_c, introduced in Section 4.3, will be considered separately for individual groups of discharges (un), (1p), (up) and (1n), as shown in Table 4.2.

It may be noticed that I_{cun}, I_{c1p}, I_{cup} and I_{c1n} are the components of the average discharge current transferred across the discharging cavity, I_c.

4.5 A NEW DEFINITION OF DISCHARGE INTENSITY

It was proposed in the preceding section that the repetition rate of internal discharges be considered separately for individual groups of discharges (un), (1p), (up) and (1n). Then, the repetition rate of unlike discharges will be equal to

$$n_u = n_{un} + n_{up} \qquad (4.9)$$

and the repetition rate of like discharges will be equal to

$$n_1 = n_{1n} + n_{1p} \qquad (4.10)$$

Table 4.1

New Proposed Indicators of Internal Partial Discharge Intensity

Indicators of	Number, Name and Symbol of Indicator
Unlike Discharges in Negative Half-Cycle (Group (un))	$\langle 1a(un)\rangle$ Apparent Charge, q_{un} $\langle 1b(un)\rangle$ Repetition Rate, n_{un} $\langle 2a(un)\rangle$ Average Discharge Current, I_{un} $\langle 2b(un)\rangle$ Quadratic Rate, D_{un} $\langle 2c(un)\rangle$ Discharge Power, P_{un}
Like Discharges in Positive Half-Cycle (Group (1p))	$\langle 1a(1p)\rangle$ Apparent Charge, q_{1p} $\langle 1b(1p)\rangle$ Repetition Rate, n_{1p} $\langle 2a(1p)\rangle$ Average Discharge Current, I_{1p} $\langle 2b(1p)\rangle$ Quadratic Rate, D_{1p} $\langle 2c(1p)\rangle$ Discharge Power, P_{1p}
Unlike Discharges in Positive Half-Cycle (Group (up))	$\langle 1a(up)\rangle$ Apparent Charge, q_{up} $\langle 1b(up)\rangle$ Repetition Rate, n_{up} $\langle 2a(up)\rangle$ Average Discharge Current, I_{up} $\langle 2b(up)\rangle$ Quadratic Rate, D_{up} $\langle 2c(up)\rangle$ Discharge Power, P_{up}
Like Discharges in Negative Half-Cycle (Group (1n))	$\langle 1a(1n)\rangle$ Apparent Charge, q_{1n} $\langle 1b(1n)\rangle$ Repetition Rate, n_{1n} $\langle 2a(1n)\rangle$ Average Discharge Current, I_{1n} $\langle 2b(1n)\rangle$ Quadratic Rate, D_{1n} $\langle 2c(1n)\rangle$ Discharge Power, P_{1n}

Table 4.2

New Proposed Quantities of Average Discharge Current
Transferred Across the Discharging Cavity in the Dielectric

Non-Measurable Quantity of	Name and Symbol of Quantity
Unlike Discharges in Negative Half-Cycle (Group (un))	Average Discharge Current Transferred Across the Discharging Cavity, I_{cun}
Like Discharges in Positive Half-Cycle (Group (1p))	Average Discharge Current Transferred Across the Discharging Cavity, I_{clp}
Unlike Discharges in Positive Half-Cycle (Group (up))	Average Discharge Current Transferred Across the Discharging Cavity, I_{cup}
Like Discharges in Negative Half-Cycle (Group (1n))	Average Discharge Current Transferred Across the Discharging Cavity, I_{cln}

It may be noticed that n_u and n_l are the components of the repetition rate, n, which is one of the most commonly used indicators of internal discharge intensity [16,18]

$$n = n_u + n_l$$

$$= n_{un} + n_{lp} + n_{up} + n_{ln} \qquad (4.11)$$

The ratio $n_u/(n_u + n_l)$ may be used to define internal partial discharge intensity. The advantages associated with the use of this definition are described in Chapters VI and VIII.

4.6   CONCLUSIONS

The presently used definitions of indicators of internal partial discharge intensity have been reviewed.

A new, nonmeasurable quantity, the average discharge current transferred across the discharging cavity has been proposed. Its value will be used in Chapter VI to check if "similar conditions" exist at all the discharging cavities belonging to a set of insulation arrangements.

Based on the identification of four groups of discharges, new indicators of discharge intensity have been proposed and a new definition of discharge intensity, the ratio $n_u/(n_u + n_l)$, has been introduced. The advantages associated with its use will be described in Chapters VI and VIII.

CHAPTER V

COMPUTATIONS OF THEORETICAL VALUES OF INDICATORS OF INTENSITY

5.1   INTRODUCTION

In this chapter the model insulation arrangement and a set of insulation arrangements are defined, which will be used to compute theoretical values of the indicators of intensity proposed in the preceding chapter.

The procedures for computing theoretical values of indicators of intensity for a set of insulation arrangements are developed. These procedures employ not only the new and more accurate pattern of recurrence, but also the commonly used pattern of recurrence. The latter procedure is developed to compare results derived from it with those using the former procedure.

Also, the method of computing breakdown voltage of air in a cavity is chosen from the methods available in literature. These methods were reviewed in Chapter II.

5.2   DETERMINATION OF MODEL INSULATION ARRANGEMENT

Theoretical computations were performed on a model arrangement of insulation. As in earlier work [8], it consists of plane layers of a solid dielectric situated between two plane electrodes. One of the internal layers has an artificial air-filled cavity of a depth t equal to a thickness of the layer and of a diameter d smaller than the diameter h of the electrodes; this ensures uniform electric field conditions in the cavity (before an inception of the first discharge in this
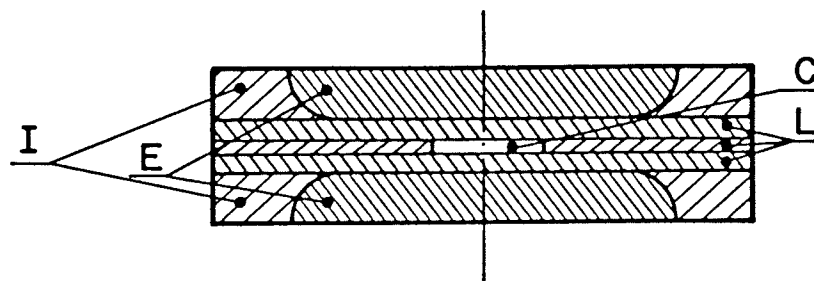
Fig. 5.1: Typical insulation arrangement:
E - electrodes; L - layers of dielectric; C - air-filled
cavity; I - auxiliary insulation.

(a) $\ell = 3$ (b) $\ell = 4$ (c) $\ell = 5$ (d) $\ell = 10$
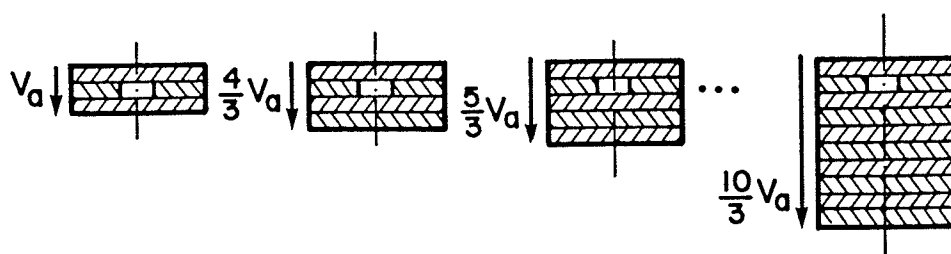
Fig. 5.2: Insulation arrangements of: a) three, b) four, c) five, and
d) ten layers of dielectric [8].

cavity). A typical insulation arrangement is shown in Fig. 5.1. The auxiliary insulation shown in Fig. 5.1 is normally used in experimental work to ensure that partial discharges do not occur adjacent to the electrodes.

Theoretical computations are carried out for insulation structures comprised of 3 or more layers. When a sufficiently high alternating voltage is applied between the electrodes, internal discharges occur in the cavity.

The voltage applied is, as in earlier work [8], increased in proportion to the number of layers, i.e. if the voltage applied to three layers is V_a, that applied to four layers is 4/3 V_a and so on. This ensures that the average electric stress between electrodes, E_{av}, will be the same for all the insulation arrangements. The average electric stress, E_{av}, is equal to the applied voltage divided by the electrode separation. It was proved, [8], that for such a case, the fictitious voltage V_c, across the cavity, in the absence of discharges, does not vary substantially for a variation of number of layers from 3 to 10. Also, it was proved as well, [8], that the number i of discharges per cycle does not vary substantially as the number of layers increases from 3 to 10. Fig. 5.2 shows the insulation arrangements and applied voltages.

Since theoretical computations are performed there is no need to consider the insulation thickness to be comprised of layers. However, for convenience of calculations, the thickness of the insulation is expressed in multiples lt of the cavity depth t. The considerations are true for bulk and layered insulation. The number of layers is varied from 3 to 129.

The capacitance C_a, Fig. 2.5, is considered to include all coupling and stray capacitances. Therefore the quantity h is not equal to the geometrical diameter of the electrode. It is assumed that the air in the cavity is at atmospheric pressure, i.e., p = 101.325 kPa. Each considered set of insulation arrangements will have only one variable quantity, namely the number of layers 1. For each set of insulation arrangements the parameters: ϵ_r, t, d, h, k, E_{av}, and f need to be specified.

5.3 PROCEDURE OF COMPUTATIONS EMPLOYING NEW PATTERN OF RECURRENCE

For each considered set of insulation arrangements the procedure using the new pattern of recurrence of internal discharges is as follows. All computations were performed using a digital computer program written in WATFIV.

For a given cavity depth the internal discharge inception voltage V_i is obtained as equal to V_{bd}, where V_{bd} is computed using the formula (2.1) from [6]. This method of computing V_{bd} was chosen as it is the most accurate from the methods available in literature.

Next, ΔV_c and V_e are computed from (2.3) and (2.4) respectively. The voltage applied to three layers, V_a, is obtained as

$$V_a = 3\, E_{av}t \qquad (5.1)$$

and its peak value is

$$\hat{V}_a = \sqrt{2}\, V_a \qquad (5.2)$$

The capacitances represented in the equivalent circuit shown in Fig. 2.5 are computed from the following formulae

$$C_c = \frac{\pi \epsilon_0 d^2}{4t} \qquad (5.3)$$

$$C_b(1) = \frac{\pi \epsilon_0 \epsilon_r d^2}{4 (1-1) t} \tag{5.4}$$

$$C_a(1) = \frac{\pi \epsilon_0 \epsilon_r (h^2 - d^2)}{41 t} \tag{5.5}$$

where: $\epsilon_0 = \frac{10^{-9}}{36 \pi} \frac{F}{m}$ is the permittivity of vacuum.

The capacitances $C_b(1)$ and $C_a(1)$ are functions of the number of layers 1. Initially a three layer dielectric, $1 = 3$, is considered and computations commence by calculating the values of the capacitances $C_b(1)$ and $C_a(1)$. For 1 layers the peak value of the applied voltage $V_a(1)$ is computed as

$$\hat{V}_a(1) = \frac{1}{3} \hat{V}_a \tag{5.6}$$

The peak value of the voltage $V_c(1)$ is obtained by substituting C_c, $C_b(1)$ and $\hat{V}_a(1)$ into (2.7)

$$\hat{V}_c(1) = \frac{C_b(1)}{C_c + C_b(1)} \hat{V}_a(1) \tag{5.7}$$

The ratios $\hat{V}_c(1)/\hat{V}_a(1)$ and $\hat{V}_c(1)/\hat{V}_a$ are also computed. The voltage drop $\Delta V_a(1)$ is obtained by substituting $C_b(1)$, $C_a(1)$ and ΔV_c into (2.8)

$$\Delta V_a(1) = \frac{C_b(1)}{C_b(1) + C_a(1)} \Delta V_c \tag{5.8}$$

The voltage gain $\Delta V_{cr}(1)$ is obtained by substituting C_c, $C_b(1)$ and $\Delta V_a(1)$ into (3.1)

$$\Delta V_{cr}(1) = \frac{C_b(1)}{C_c + C_b(1)} \Delta V_a(1) \tag{5.9}$$

The voltage drop $\Delta V_{ct}(1)$ is obtained by substituting ΔV_c and $\Delta V_{cr}(1)$ into (3.3)

$$\Delta V_{ct}(1) = \Delta V_c - \Delta V_{cr}(1) \tag{5.10}$$

It follows from (3.3) that the voltage $V_r(1)$ is equal to

$$V_r(1) = V_i - \Delta V_{ct}(1) \qquad (5.11)$$

It follows from (3.4) and (3.5) that the number $m(1)$ of internal discharges per quarter-cycle of alternating voltage is the largest integer which satisfies

$$m(1) \leq \frac{\hat{V}_c(1) - V_r(1)}{\Delta V_{ct}(1)} = R(1) \qquad (5.12)$$

where $R(1)$ is the reference number as a function of 1.

The numbers of discharges per half-cycle, $j(1)$, per cycle, $i(1)$, and per second, $n(1)$, are then computed from the following formulae

$$j(1) = 2m(1) \qquad (5.13)$$

$$i(1) = 4m(1) \qquad (5.14)$$

$$n(1) = 4fm(1)$$

$$= fi(1) \qquad (5.15)$$

In general, the magnitudes of individual discharges differ. However, on the basis of the equivalent circuit of Fig. 2.5, with the assumption that $\Delta V_c^+ = \Delta V_c^-$, all the discharges are of equal magnitude and the apparent charge $q(1)$ is equal to

$$q(1) = [C_a(1) + \frac{C_c C_b(1)}{C_c + C_b(1)}] \Delta V_a(1) \qquad (5.16)$$

Similarly, the charge $q_c(1)$ actually transferred across the discharging cavity is equal to

$$q_c(1) = [C_c + \frac{C_b(1) C_a(1)}{C_b(1) + C_a(1)}] \Delta V_c \qquad (5.17)$$

Therefore, theoretically, the apparent charge has the same value $q(1)$ for each of the four groups of discharges (un), (1p), (up) and

(1n), presented in Table 4.1. Hence, q(1) needs to be computed only once. This is also true for the charge $q_c(1)$ actually transferred across the discharging cavity, and therefore this is true as well for the charge ratio $q(1)/q_c(1)$ and for the squared apparent charge, $[q(1)]^2$.

As in [2], it may be obtained, using (5.10), (5.16) and (5.17), that the charge ratio $q(1)/q_c(1)$ is equal to

$$\frac{q(1)}{q_c(1)} = \frac{C_b(1)}{C_c + C_b(1)} \qquad (5.18)$$

and is independent of the capacitance $C_a(1)$.

Using (5.3) and (5.4) in (5.18) it may be obtained that [2]

$$\frac{q(1)}{q_c(1)} = \frac{\epsilon_r}{\epsilon_r + 1 - 1} \qquad (5.19)$$

The squared apparent charge, $[q(1)]^2$, is equal to

$$[q(1)]^2 = [C_a(1) + \frac{C_c C_b(1)}{C_c + C_b(1)}]^2 [\Delta V_a(1)]^2 \qquad (5.20)$$

In general, the numbers of discharges in individual groups (un), (1p), (up) and (1n), shown in Fig. 3.3 and in Table 4.1, are all different. However, on the basis of the equivalent circuit of Fig. 2.5, with the assumption made that V_i and V_e are polarity independent, it is obtained that V_r also is polarity independent. Therefore, as can be seen from Fig. 3.3, the group (up) is a "mirror image" of the group (un), and the group (1n) is a "mirror image" of the group (1p). Hence, the theoretical analysis of individual discharges needs to be carried out for two groups only, such as (un) and (1p). Therefore, half-cycles, between 270° el and 450° el in Fig. 3.3, are analyzed. The computer program written in WATFIV analyzes j(1) discharges in such a half-

cycle. It determines for each kth discharge the instantaneous value $V_{ck}(1)$ of the voltage $V_c(1)$ and the instantaneous value $U_k(1)$ of the applied voltage $V_a(1)$. If the value of $U_k(1)$ is negative, the discharge is classified as an unlike discharge occurring in the negative half-cycle - group (un); if the value of $U_k(1)$ is positive or zero, the discharge is classified as a like discharge occurring in the positive half-cycle - group (1p). The sums of the values of $U_k(1)$ are computed separately for group (un) and group (1p). The numbers of discharges per half-cycle in group (un), $j_{un}(1)$, and in group (1p), $j_{1p}(1)$, are also computed.

The numbers of discharges per cycle in group (un), $i_{un}(1)$, and in group (1p), $i_{1p}(1)$, are respectively

$$i_{un}(1) = j_{un}(1) \tag{5.21}$$
$$i_{1p}(1) = j_{1p}(1) \tag{5.22}$$

The repetition rates of group (un), $n_{un}(1)$, and of group (1p), $n_{1p}(1)$, are respectively

$$n_{un}(1) = f i_{un}(1) \tag{5.23}$$
$$n_{1p}(1) = f i_{1p}(1) \tag{5.24}$$

Since all discharges are of equal magnitude, the discharge powers of group (un), $P_{un}(1)$, and of group (1p), $P_{1p}(1)$, are computed from simplified formulae

$$P_{un}(1) = \frac{1}{T} q(1) \ \Sigma U_{kun}(1)$$

$$= fq(1) \ \Sigma U_{kun}(1) \tag{5.25}$$

$$P_{1p}(1) = \frac{1}{T} q(1) \ \Sigma U_{kun}(1)$$

$$= fq(1) \ \Sigma U_{kun}(1) \tag{5.26}$$

Since all discharges are of equal magnitude, the average discharge currents of group (un), $I_{un}(1)$, and of group (1p), $I_{1p}(1)$, and the quadratic rates of group (un), $D_{un}(1)$, and of group (1p), $D_{1p}(1)$, and also the average discharge currents transferred across the discharging cavity of group (un), $I_{cun}(1)$, and of group (1p), $I_{c1p}(1)$, are all computed from simplified formulae and are respectively

$$I_{un}(1) = n_{un}(1) \ q(1) \qquad (5.27)$$

$$I_{1p}(1) = n_{1p}(1) \ q(1) \qquad (5.28)$$

$$D_{un}(1) = n_{un}(1) \ [q(1)]^2 \qquad (5.29)$$

$$D_{1p}(1) = n_{1p}(1) \ [q(1)]^2 \qquad (5.30)$$

$$I_{cun}(1) = n_{un}(1) \ q_c(1) \qquad (5.31)$$

$$I_{c1p}(1) = n_{1p}(1) \ q_c(1) \qquad (5.32)$$

The following statements are true for the indicators and quantities presented in Tables 4.1 and 4.2: those of group (up) are equal to their correspondents of group (un), and those of group (1n) are equal to their correspondents of group (1p).

Therefore the total indicators, which are presently in use, are expressed in terms of the proposed new indicators as follows:

$$n(1) = 2 \ [n_{un}(1) + n_{1p}(1)] \qquad (5.33)$$

$$I(1) = 2 \ [I_{un}(1) + I_{1p}(1)] \qquad (5.34)$$

$$D(1) = 2 \ [D_{un}(1) + D_{1p}(1)] \qquad (5.35)$$

$$P(1) = 2 \ [P_{un}(1) + P_{1p}(1)] \qquad (5.36)$$

Similarly, the total new nonmeasurable quantity, $I_c(1)$, can be expressed in terms of its proposed components as

$$I_c(1) = 2 \ [I_{cun}(1) + I_{c1p}(1)] \qquad (5.37)$$

This total average discharge current transferred across the dis-

charging cavity is used as a criterion to check if "similar conditions" exist in the cavity, which has the same dimensions for the whole considered set of insulation arrangements.

Since $n_{up}(1) = n_{un}(1)$ and $n_{ln}(1) = n_{lp}(1)$, the repetition rates of unlike discharges, $n_u(1)$, and of like discharges, $n_l(1)$, are computed as

$$n_u(1) = n_{un}(1) + n_{up}(1)$$

$$= 2\, n_{un}(1) \qquad\qquad (5.38)$$

$$n_l(1) = n_{ln}(1) + n_{lp}(1)$$

$$= 2\, n_{lp}(1) \qquad\qquad (5.39)$$

The function $n_u(1)/[n_u(1) + n_l(1)]$ introduced as a new definition of internal partial discharge intensity is computed next.

After computing $n_u(1)/[n_u(1) + n_l(1)]$ the computer program jumps to the next number of layers 1 and proceeds as before until the computations are completed.

5.4   COMPARISON WITH PROCEDURE OF COMPUTATIONS EMPLOYING COMMONLY USED PATTERN OF RECURRENCE

In addition to the computations employing the new pattern of recurrence of internal discharges, the computations employing the commonly used pattern of recurrence were also performed for comparison. For each considered set of insulation arrangements these computations proceed in a manner similar to that outlined in Section 5.3. All the computations were performed using another computer program written in WATFIV. This program has many common steps with the program presented in Section 5.3. A comparison of these two programs showing the differences that

exist between computations employing the two different patterns of recurrence will be outlined below.

The computations initially proceed as in Section 5.3 using formulae (5.1)-(5.8). Since the voltage gain $\Delta V_{cr}(1)$ is not considered here, the next step is the determination of the number $m^*(1)$ of internal discharges per quarter-cycle of alternating voltage.

It follows from (2.5) and (2.6) that the number $m^*(1)$ is the largest integer which satisfies

$$m^*(1) \leq \frac{\hat{V}_c(1) - V_e}{\Delta V_c} = R^*(1) \tag{5.40}$$

where $R^*(1)$ is the reference number as a function of 1.

The numbers of discharges per half-cycle, $j(1)$, per cycle, $i(1)$, and per second, $n(1)$, are given here by the following formulae

$$j(1) = 2m^*(1) \tag{5.41}$$

$$i(1) = 4m^*(1) \tag{5.42}$$

$$n(1) = 4fm^*(1)$$

$$= fi(1) \tag{5.43}$$

which, in general, do not yield the same values as the formulae (5.13), (5.14) and (5.15) respectively.

Next, the computations proceed as in Section 5.3 using formulae (5.16)-(5.39) with the only difference that the analysis of $j(1)$ discharges in the half-cycle yields, in general, different instantaneous values $V_{ck}(1)$ and $U_k(1)$ from those obtained in Section 5.3. Furthermore, in general, all computed numbers of discharges are different from those obtained in Section 5.3.

Therefore, in general, the values of all the indicators and quanti-

ties expressed by formulae (5.23)-(5.39) are different from those obtained in Section 5.3.

The criterion for checking if "similar conditions" exist at the discharge site is the same as the one used in Section 5.3; the computations continue in the same manner as in Section 5.3.

5.5   CONCLUSIONS

The model insulation arrangement has been defined. Each arrangement consists of one air-filled cavity, which is disc shaped with the diameter of the disc exceeding its thickness. The electric field in the cavity is uniform. Such a choice is justified from three points of view. First, it is important to carry out such studies under uniform field conditions. Secondly, it allows the calculation of the inception voltage for the cavity with good accuracy. Lastly, the electric stress concentration factor for such cavities is equal to the relative permittivity of the solid insulation and is higher than the factor which is obtained with either a spherical cavity or a disc shaped cavity whose thickness exceeds its diameter.

A set of insulation arrangements has been defined. The average electric stress is the same for all the cases considered. The usefulness of the definition of a set will be demonstrated in the next chapter.

Two procedures of computations of theoretical values of indicators of intensity for a set of insulation arrangements have been developed. The first procedure employs the new and more accurate pattern of recurrence. The second procedure, employing the commonly used pattern of

recurrence, is used to compare its results with those of the first procedure.

From the methods available in literature an accurate method has been chosen to compute the breakdown voltage of air in a cavity.

CHAPTER VI

EVALUATION OF INDICATORS OF DISCHARGE INTENSITY

6.1   INTRODUCTION

In this chapter the results of computations, carried out on a digital computer, are presented for a typical set of insulation arrangements. The computations follow the two procedures described in the preceding chapter. First, the results of computations employing the new pattern are presented. Next, those employing the commonly used pattern are shown for comparison. In both cases, the definition of a set produces "similar conditions" at all the discharging cavities belonging to a set.

In this thesis the risk of insulation failure means the likelihood that an insulation will have a lifetime shorter than the expected lifetime for that insulation.

"Similar conditions" at the discharge site mean that the average discharge current transferred across the discharging cavity, I_c, shows a relatively small variation as the number of layers of a solid dielectric, l, increases from 3 to 129, i.e., forty three times.

In this thesis a stable indicator means the indicator which shows a relatively small variation as the number of layers of a solid dielectric, l, varies in a set of insulation arrangements. On the other hand, an unstable indicator means the indicator which shows a significant variation as the number of layers of a solid dielectric, l, varies in a set of insulation arrangements.

Since "similar conditions" exist at the discharge site in a set of

insulation arrangements, a desired indicator is a stable one. It may be noted that generally a stable indicator fits the production line test of an equipment, whereas an unstable indicator fits an in situ test of an equipment in service.

In this thesis a more conservative assessment of the risk of insulation failure means larger values of the indicators n, I, D, P, n_u, n_1 and $n_u/(n_u + n_1)$.

The results of computations show that there are, in some cases very serious, disadvantages associated with the application of the commonly used indicators of intensity, and that a new proposed definition of intensity, as an indicator, is relatively free of these disadvantages. A comparison of the results of computations employing two different patterns of recurrence shows that when the repetition rate or a quantity derived from it is used as an indicator, the new and more accurate pattern leads, in general, to a more conservative assessment of the risk of insulation failure than the commonly used pattern does.

6.2   RESULTS OF COMPUTATIONS EMPLOYING NEW PATTERN OF RECURRENCE

The computations employing the new pattern of recurrence, which were carried out on a digital computer, followed the procedure defined in Section 5.3. Tables 6.1-6.3 show the results of computations for a typical set of insulation arrangements with parameters as indicated. Similar results were obtained for other typical values of the parameters ϵ_r, t, d, h, k, E_{av} and f.

Table 6.1 shows the results of computations of discharge intensity obtained by the application of the new definition, the ratio $n_u/(n_u +$

Table 6.1

Results of Computations of Indicators of Discharge Intensity
Employing New Pattern of Recurrence;
ϵ_r = 2.3, t = 36 μm, d = 10 mm, h = 40 mm,
k = 0.3, E_{av} = 13.1 kV/mm, f = 60 Hz

l	I_c	q	q_c	$\dfrac{q}{q_c}$	n	n_u	n_l	$\dfrac{n_u}{n_u + n_l}$
[-]	[μA]	[pC]	[pC]	[-]	[s^{-1}]	[s^{-1}]	[s^{-1}]	[-]
3	7.404	2750	5141	0.5349	1440	360	1080	0.250
5	6.464	1405	3848	0.3651	1680	480	1200	0.286
9	6.117	711	3186	0.2233	1920	600	1320	0.313
17	5.474	358	2851	0.1257	1920	600	1320	0.313
33	5.795	180	2683	0.0671	2160	720	1440	0.333
65	5.162	90	2598	0.0347	2160	720	1440	0.333
129	5.521	45	2556	0.0177	2160	720	1440	0.333

Table 6.2

Results of Computations Employing New Pattern of Recurrence;
$\epsilon_r = 2.3$, $t = 36$ μm, $d = 10$ mm, $h = 40$ mm,
$k = 0.3$, $E_{av} = 13.1$ kV/mm, $f = 60$ Hz

l	R	n	n_{un}	m_{lp}	l	I_{un}	I_{lp}	D	D_{un}	D_{lp}	P	P_{un}	P_{lp}	I_c	I_{cun}	I_{clp}
[-]	[-]	[s^{-1}]	[s^{-1}]	[s^{-1}]	[μA]	[μA]	[μA]	[$\frac{(nC)^2}{s}$]	[$\frac{(nC)^2}{s}$]	[$\frac{(nC)^2}{s}$]	[mW]	[mW]	[mW]	[μA]	[μA]	[μA]
3	6.129	1440	180	540	3.960	0.495	1.485	10890.75	1361.34	4084.03	2.757	-0.172	1.550	7.404	0.925	2.776
5	7.183	1680	240	600	2.360	0.337	0.843	3315.12	473.59	1183.97	2.398	-0.242	1.441	6.464	0.923	2.309
9	8.063	1920	300	660	1.366	0.213	0.470	971.71	151.83	334.02	2.265	-0.320	1.453	6.117	0.956	2.103
17	8.666	1920	300	660	0.688	0.107	0.236	246.52	38.52	84.74	2.024	-0.292	1.304	5.474	0.856	1.882
33	9.027	2160	360	720	0.389	0.065	0.130	69.90	11.65	23.30	2.141	-0.395	1.465	5.795	0.966	1.932
65	9.226	2160	360	720	0.195	0.032	0.065	17.55	2.92	5.85	2.073	-0.384	1.421	5.162	0.935	1.871
129	9.331	2160	360	720	0.097	0.016	0.032	4.40	0.73	1.47	2.039	-0.379	1.398	5.521	0.920	1.840

Table 6.3

Computed Quantities Which are Identical
Employing Either Pattern of Recurrence;
$\epsilon_r = 2.3$, $t = 36 \,\mu m$, $d = 10$ mm, $h = 40$ mm,
$k = 0.3$, $E_{av} = 13.1$ kV/mm, $f = 60$ Hz

l	$\hat{V}_c$	q	q_c	$\dfrac{q}{q_c}$	q^2
[-]	[V]	[pC]	[pC]	[-]	$[(nC)^2]$
3	1070.2	2750	5141	0.5349	7.5630
5	1217.4	1405	3848	0.3651	1.9733
9	1340.4	711	3186	0.2233	0.5061
17	1425.0	358	2851	0.1257	0.1284
33	1475.8	180	2683	0.0671	0.0324
65	1503.9	90	2598	0.0347	0.0081
129	1518.7	45	2556	0.0177	0.0020

n_l). Also, the values of the component indicators, n_u and n_l, of the new definition, the values of the two commonly used indicators q and n, and of the quantities I_c, q_c and q/q_c are shown in Table 6.1.

Table 6.2 shows the results of computations of new proposed and existing indicators of discharge intensity, and of quantities as indicated.

The computed quantities which are identical employing either pattern of recurrence are shown in Table 6.3.

It is seen from Table 6.1 that for a very large variation of 1, from 3 to 129, the values of I_c vary between 5.162 and 7.404 μA only. Furthermore, no definite trend is exhibited in this variation. Therefore, I_c may be considered to have similar values as 1 varies from 3 to 129. Thus the conditions at the discharge site may be considered to be similar.

Table 6.1 also shows that the apparent charge, q, one of the most commonly used indicators of internal discharge intensity [16-18], decreases to less than one sixtieth of its initial value as 1 increases from 3 to 129. As an indicator, q is therefore very unstable. In contrast, the new definition, the ratio $n_u/(n_u + n_l)$ is stable as an indicator; its value varies from 0.250 to 0.333, an increase of about 33%, as 1 increases from 3 to 129.

Of the three remaining indicators n, n_u and n_l, n_l shows a variation similar to that of $n_u/(n_u + n_l)$. Both n and n_u show a greater variation. The commonly used indicator, n, exhibits a variation of 50%, whereas n_u exhibits a variation of 100%.

It can therefore be concluded that $n_u/(n_u + n_l)$ and n_l are the two

most stable indicators and are much more stable than the apparent charge q.

Another interesting fact emerges from an examination of the results in Table 6.1. As l varies from 3 to 129, q_c decreases by only about 50% from 5141 to 2556 pC. On the other hand, as pointed out earlier, the decrease in q is comparatively large. For the same variation in l, q decreases from a value of 2750 to 45 pC. This clearly shows that the use of apparent charge, as an indicator, results in an underestimation of the risk of insulation failure when the amount of charge q_c actually transferred at the discharge location is large compared to the measured apparent charge q. Table 6.1 shows that the underestimation of risk becomes more pronounced for large l; the ratio q/q_c becomes very small for large l. On the other hand, the new definition, the ratio $n_u/(n_u + n_l)$, is sensibly constant as an indicator and therefore does not underestimate the risk of insulation failure.

The fact that the measured apparent charge q may be in some cases, as for large l in Table 6.1, several orders of magnitude different from the amount of charge q_c actually transferred at the discharge site has been recognized for some time [19]. The problems of apparent charge measurements were recently summarized in [19].

It is seen from Table 6.2 that as l varies from 3 to 129, the components of n, i.e., n_{un} and n_{lp} exhibit variations similar to those of n_u and n_l respectively. Two latter variations as well as a variation of n were discussed earlier in this section, Table 6.1.

Table 6.2 also shows that the indicator I decreases to less than one fortieth of its initial value as l increases from 3 to 129. As an

indicator, I is therefore very unstable. Its components I_{un} and I_{1p} decrease to less than one thirtieth and less than one fortieth of their initial values respectively, as 1 varies from 3 to 129. They too are very unstable as indicators.

It is seen from Table 6.2 that the indicator D decreases to less than one two thousandth of its initial value for a variation of 1 from 3 to 129. As an indicator, D is therefore exceptionally unstable. Its components D_{un} and D_{1p} decrease to about one two thousandth and less than one two thousandth of their initial values respectively, as 1 varies from 3 to 129. They too are exceptionally unstable as indicators.

It can therefore be concluded that $n_u/(n_u + n_1)$ and n_1, as the two most stable indicators, are much more stable than the average discharge current I and the quadratic rate D.

Table 6.2 also shows that for a variation of 1 from 3 to 129, the values of P vary between 2.024 and 2.757 mW only. Furthermore, no definite trend is exhibited in this variation. Since the discharge power P is related to the degradation rate of the insulation subjected to discharges, a relatively small variation in P seems to confirm the validity of using I_c to ascertain whether similar conditions exist at the discharge sites in a set of insulation arrangements. Table 6.2 shows that as an indicator, P is stable; its value varies about 36% as 1 varies from 3 to 129. It is also seen from Table 6.2 that no definite trend is exhibited in a variation of either component of P, i.e., P_{un} or P_{1p}, as 1 increases from 3 to 129. For this variation of 1, P_{un} varies between -0.172 and -0.395 mW, a variation of about 130%, whereas P_{1p} varies between 1.304 and 1.550 mW only, a variation of about 19%.

Therefore, of the three indicators P, P_{un} and P_{1p}, P_{1p} shows a smaller variation than that of P, whereas P_{un} shows a greater variation than that of P. Hence, as an indicator P_{1p} is stable. It may be noticed that the values of P_{un} are negative which means that the energy flow associated with unlike discharges in the negative half-cycle is directed from the insulation to the voltage source. Also, the energy flow associated with unlike discharges in the positive half-cycle is directed from the insulation to the voltage source.

It may be noticed that P_{1n} is equal to P_{1p}, since P_{1n} is the correspondent of P_{1p}. It can therefore be concluded that the discharge power of like discharges, P_1, which is the sum of P_{1n} and P_{1p}, and is the component of the discharge power P, is also stable as an indicator. However, as may be noticed from formula (4.6), the practical measurement of the indicator P, and its component of like discharges, P_1, is more difficult than the practical measurement of the new indicator, $n_u/(n_u + n_1)$. It may be seen from formula (4.6) that the measurement of P or P_1 requires the recording of the values of q_k and U_k for each kth discharge considered. It is very difficult to do so with good accuracy. On the other hand, the measurement of $n_u/(n_u + n_1)$ requires the recording of the repetition rates n_u and n_1 only. It is relatively easy to do so with very good accuracy.

It can therefore be concluded that the new definition of discharge intensity, the ratio $n_u/(n_u + n_1)$, which is stable as an indicator, is easier to measure than the stable indicators, the discharge power P and its component of like discharges P_1. Similarly, the indicator n_1 is easier to measure than P and P_1.

It is seen from Table 6.3 that the fictitious voltage across the cavity in the absence of discharges, $\hat{V}_C$, increases by only about 40% from 1070.2 to 1518.7 V, as 1 varies from 3 to 129. Thus the quantity $\hat{V}_C$ is sensibly stable, which further strengthens the validity of checking that "similar conditions" do exist at all the cavities belonging to a set of insulation arrangements defined in Chapter V.

Table 6.3 also shows that the squared apparent charge, q^2, decreases to less than one three thousandth of its initial value as 1 increases from 3 to 129. As an indicator, q^2 is therefore exceptionally unstable.

It can therefore be concluded that $n_u/(n_u + n_1)$ and n_1, as the two most stable indicators, are much more stable than the squared apparent charge, q^2.

Another interesting fact emerges from an examination of the results in Table 6.2. As 1 varies from 3 to 129, the reference number R increases by about 50% from 6.129 to 9.331. This increase is similar to that of the repetition rate n. However, as one may also deduce from inequality (5.12), the variation of R is smoother than that of n.

6.3   COMPARISON WITH RESULTS OF COMPUTATIONS
EMPLOYING COMMONLY USED PATTERN OF RECURRENCE

The computations employing the commonly used pattern of recurrence, which were carried out on a digital computer, followed the procedure defined in Section 5.4. These computations were performed for comparison of the results obtained with those employing the new pattern of recurrence. The results of the latter computations have been included

in the preceding section. Tables 6.4 and 6.5 show the results of computations, employing the commonly used pattern of recurrence, for the same typical set of insulation arrangements as considered in the preceding section, Tables 6.1-6.3. All parameters indicated in Tables 6.4 and 6.5 are identical to those in Tables 6.1-6.3. Similar results were obtained for other typical values of the parameters ϵ_r, t, d, h, k, E_{av} and f.

Comparing the results shown in Table 6.4 with their correspondents which were shown in Table 6.1 in the preceding section, one notices that as l varies from 3 to 129, the quantity I_c^*, and the indicators n^*, n_u^*, n_l^* and $n_u^*/(n_u^* + n_l^*)$ exhibit variations similar to those described in the preceding section for their correspondents I_c, n, n_u, n_l and $n_u/(n_u + n_l)$ respectively. As pointed out in the preceding section, Table 6.3, certain quantities are identical employing either pattern of recurrence. These are the voltage $\hat{V}_c$, the charges q and q_c, and the charge ratio q/q_c. Therefore, as l varies from 3 to 129, the indicator q^*, and the quantities q_c^* and q^*/q_c^*, shown in Table 6.4, exhibit variations identical to those described in the preceding section, Table 6.1, for their identical correspondents q, q_c and q/q_c respectively. Also, the variation shown by V_c as l increases from 3 to 129, which was described in the preceding section, Table 6.3, is valid for the commonly used pattern of recurrence as well.

Comparing the results shown in Table 6.5 with their correspondents which were shown in Table 6.2 in the preceding section, it may be seen that as l increases from 3 to 129, the quantities R^*, n^*, n_{un}^*, n_{lp}^*, I^*, I_{un}^*, I_{lp}^*, D^*, D_{un}^*, D_{lp}^*, P^*, P_{un}^*, P_{lp}^*, I_c^*, I_{cun}^* and I_{clp}^* exhibit variations similar to those described in the preceding section

Table 6.4

Results of Computations of Indicators of Discharge Intensity
Employing Commonly Used Pattern of Recurrence;
$\epsilon_r = 2.3$, $t = 36\ \mu m$, $d = 10$ mm, $h = 40$ mm,
$k = 0.3$, $E_{av} = 13.1$ kV/mm, $f = 60$ Hz

l	$I_c^\star$	$q^\star$	$q_c^\star$	$\dfrac{q^\star}{q_c^\star}$	$n^\star$	$n_u^\star$	$n_l^\star$	$\dfrac{n_u^\star}{n_u^\star + n_l^\star}$
[-]	[μA]	[pC]	[pC]	[-]	[s^{-1}]	[s^{-1}]	[s^{-1}]	[-]
3	6.170	2750	5141	0.5349	1200	240	960	0.200
5	6.464	1405	3848	0.3651	1680	480	1200	0.286
9	5.352	711	3186	0.2233	1680	480	1200	0.286
17	5.474	358	2851	0.1257	1920	600	1320	0.313
33	5.151	180	2683	0.0671	1920	600	1320	0.313
65	5.612	90	2598	0.0347	2160	720	1440	0.333
129	5.521	45	2556	0.0177	2160	720	1440	0.333

Table 6.5

Results of Computations Employing Commonly Used Pattern of Recurrence;
$\epsilon_r = 2.3$, $t = 36\ \mu m$, $d = 10$ mm, $h = 40$ mm,
$k = 0.3$, $E_{av} = 13.1$ kV/mm, $f = 60$ Hz

l	R^*	n^*	n_{un}^*	m_{lp}^*	I^*	I_{un}^*	I_{lp}^*	D^*	D_{un}^*	D_{lp}^*	P^*	P_{un}^*	P_{lp}^*	I_c^*	I_{cun}^*	I_{clp}^*
[-]	[-]	$[s^{-1}]$	$[s^{-1}]$	$[s^{-1}]$	$[\mu A]$	$[\mu A]$	$[\mu A]$	$\frac{(nC)^2}{s}$	$\frac{(nC)^2}{s}$	$\frac{(nC)^2}{s}$	[mW]	[mW]	[mW]	$[\mu A]$	$[\mu A]$	$[\mu A]$
3	5.880	1200	120	480	3.300	0.330	1.320	9075.62	907.56	3630.25	2.278	-0.094	1.233	6.170	0.617	2.468
5	7.010	1680	240	600	2.360	0.337	0.843	3315.12	473.59	1183.97	2.387	-0.261	1.454	6.464	0.923	2.309
9	7.953	1680	240	600	1.195	0.171	0.427	850.24	121.46	303.66	1.976	-0.216	1.204	5.352	0.765	1.912
17	8.602	1920	300	660	0.688	0.107	0.236	246.52	38.52	84.74	2.020	-0.297	1.308	5.474	0.856	1.882
33	8.992	1920	300	660	0.345	0.054	0.119	62.13	9.71	21.36	1.902	-0.280	1.230	5.151	0.805	1.771
65	9.208	2160	360	720	0.195	0.032	0.065	17.55	2.92	5.85	2.072	-0.386	1.422	5.612	0.935	1.871
129	9.321	2160	360	720	0.097	0.016	0.032	4.40	0.73	1.47	2.038	-0.380	1.399	5.521	0.920	1.840

for their correspondents R, n, n_{un}, n_{1p}, I, I_{un}, I_{1p}, D, D_{un}, D_{1p}, P, P_{un}, P_{1p}, I_c, I_{cun} and I_{c1p} respectively. However, in this case, where the commonly used pattern of recurrence is employed, the fact that the variation of R* is smoother than that of n* may be deduced from inequality (5.40).

Another interesting fact emerges from a comparison of the results of R, Table 6.2, with those of R*, Table 6.5. It may be noticed that for any tabulated value of 1, the computed value of R is always greater than that of its correspondent R*. It may also be noticed that the difference between these corresponding values of R and R* decreases as 1 increases from 3 to 129. This difference for 1 = 3 is equal to 0.239, whereas for 1 = 129 it is equal to only 0.010.

As one may notice from inequalities (5.12) and (5.40), even a very small difference between R and R* may cause a difference between the repetition rates n and n*. This, indeed is the case of 1 equal to 33, where R equals 9.027, Table 6.2, and R* equals 8.992, Table 6.5, the difference of 0.035 only. However, the repetition rates for 1 equal to 33 differ, since n equals 2160 s^{-1}, Table 6.2, and n* equals 1920 s^{-1}, Table 6.5.

It may therefore be concluded that since the computed value of R is always greater than that of its correspondent R*, the values of the repetition rate n, and the derived indicators I, D, P and the quantity I_c, computed by employing the new pattern, are always greater than or equal to the values of their correspondents n*, I*, D*, P* and I_c* respectively, computed by employing the commonly used pattern. Comparing the values of n, I, D, P and I_c, Table 6.2, with those of their corres-

pondents n^*, I^*, D^*, P^* and I_c^* respectively, Table 6.5, one may notice that the above statement is true for all corresponding pairs of tabulated values, one taken from Table 6.2, the other from Table 6.5. An example of this has been shown in the preceding paragraph for the value of n and that of its correspondent n^* for the case of l equal to 33.

Since the new and more accurate pattern of recurrence of discharges yields the values of indicators n, I, D and P which are greater than or equal to those obtained by the application of the commonly used pattern of recurrence, it may be concluded that, when the repetition rate n or a quantity derived from it I, D or P is used as an indicator, the new pattern leads, in general, to a more conservative assessment of the risk of insulation failure than the commonly used pattern does. It may be noted however that the indicators do not depend strongly on the choice of a pattern of recurrence.

It may also be noted that the procedures of computations have been developed on the basis of the commonly used equivalent circuit of the dielectric, shown in Fig. 2.5. However, that circuit does not explain fully the behaviour of internal partial discharges. For instance, in practice, when measuring the apparent charge, one obtains a distribution of many values [1,8,13,20,21,22,23,24,25,26]. The equivalent circuit does not yield this distribution and the apparent charge has the same value for all discharges.

6.4   CONCLUSIONS

The results of computations, carried out on a digital computer, have been presented for a typical set of insulation arrangements. The

computations followed the two procedures described in the preceding chapter. First, the results of computations employing the new pattern of recurrence of discharges have been presented. Next, those employing the commonly used pattern of recurrence of discharges have been shown for comparison. In both cases, it has been pointed out that the definition of a set produces "similar conditions" at all the discharging cavities belonging to a set.

It has been shown that for "similar conditions" existing at the discharge site i.e. similar values of the average discharge current transferred across the discharging cavity, I_c, significant differences are obtained in the theoretical values of a presently used indicator of discharge intensity, the apparent charge q. These significant differences are also obtained for the indicator I, the average discharge current, and are even more pronounced for the indicator D, the quadratic rate, and for the quantity q^2, the squared apparent charge. On the other hand, the theoretical values of the new proposed definition of discharge intensity, the ratio $n_u/(n_u + n_1)$, do not differ significantly.

As indicators, the quantities $n_u/(n_u + n_1)$ and n_1 are two most stable ones, being more stable than the quantities n and n_u. The advantages associated with the use of the new indicator $n_u/(n_u + n_1)$ over the use of the indicators n_1, n and n_u will be explained in Chapter VIII.

The indicators $n_u/(n_u + n_1)$ and n_1 are easier to measure than the other two stable indicators, the discharge power, P, and its component of like discharges, P_1. It has been explained that it is relatively

easy to perform the practical measurements of $n_u/(n_u + n_l)$ and n_l with very good accuracy, whereas it is very difficult to perform the practical measurements of P and P_l with good accuracy.

The apparent charge q often underestimates the risk of insulation failure, whereas the new indicator $n_u/(n_u + n_l)$ does not do so.

The values of the discharge power of unlike discharges in the negative half-cycle, P_{un}, are negative which means that the energy flow associated with unlike discharges in the negative half-cycle is directed from the insulation to the voltage source. Also, the energy flow associated with unlike discharges in the positive half-cycle is directed from the insulation to the voltage source.

The voltage $\hat{V}_c$, the charges q and q_c, and the charge ratio q/q_c are the quantities which are identical employing either pattern of recurrence. For all other tabulated quantities: n, n_u, n_l, n_{up}, n_{lp}, I, I_{un}, I_{lp}, D, D_{un}, D_{lp}, P, P_{un}, P_{lp}, I_c, I_{cun}, I_{clp}, and R, it has been shown that their variations with 1 according to the new pattern are similar to those of their correspondents according to the commonly used pattern: n^*, n_u^*, n_l^*, n_{up}^*, n_{lp}^*, I^*, I_{un}^*, I_{lp}^*, D^*, D_{un}^*, D_{lp}^*, P^*, P_{un}^*, P_{lp}^*, I_c^*, I_{cun}^*, I_{clp}^*, and R^*, respectively.

It has been concluded from a comparison of the results of computations employing two different patterns of recurrence that when the repetition rate or a quantity derived from it I, D or P is used as an indicator, the new and more accurate pattern leads, in general, to a more conservative assessment of the risk of insulation failure than the commonly used pattern does. It may be noted however that the indicators do not depend strongly on the choice of a pattern of recurrence.

The procedures of computations were developed on the basis of the commonly used equivalent circuit, Fig. 2.5, which, however, does not explain fully the behaviour of discharges. Therefore, a comparison of the results of computations with recently published experimental results, for insulation arrangements identical to the one considered in this thesis, will be presented in the next chapter.

CHAPTER VII

COMPARISON OF RESULTS
OF COMPUTATIONS WITH PUBLISHED EXPERIMENTAL RESULTS

7.1   INTRODUCTION

In this chapter the results of computations are compared with experimental results, published in recent literature [20-22], obtained using laboratory model insulation arrangements identical to the one considered in this thesis. The procedure of computations employing the new and more accurate pattern of recurrence of discharges is used.

Reasonable agreement is found between experimental and computed values of the apparent charge q, the repetition rate n and the distribution of discharge pulses [20-22]. Several examples of this agreement are shown.

7.2   COMPARISON OF RESULTS

Experimental values of the apparent charge q, the repetition rate n and the distribution of discharge pulses, obtained using insulation arrangements identical to the one considered in this thesis, have been reported in recent literature [20-22]. Theoretical computations, employing the new pattern of recurrence, were performed on these insulation arrangements. Several typical examples of a comparison of the results of these computations with the experimental results are presented below.

The value of the discharge coefficient k, $k = (V_i - V_e)/V_i$, for a typical insulation is most often reported in the literature [1,2,4,7,8, 13,14,22] within the range between 0.1 and 0.5, with the average of 0.3

used in analytical studies. Of the three considered in this section experimental studies [20-22], in two, [20,21], the value of k has not been reported. Therefore, the average value of k = 0.3 was assumed in theoretical computations for the insulation arrangements from the studies [20,21]. In the experimental study [22] the value of k has been reported as presumed to be 0.5.

Table 7.1 shows a comparison of the results of theoretical computations with the experimental results published in recent literature [20], for the apparent charge q, with parameters as indicated. The experimental frequency f varied from 0.1 to 50 Hz [20]. The theoretically computed values of the apparent charge q are independent of the frequency f.

It is seen from Table 7.1 that the computed values of q, which correspond to average values, agree reasonably with the experimental values of q. For each value of the diameter of the cavity d, Table 7.1, the computed value is always smaller than the experimental peak value and is not much different from the experimental most probable value. For example, for d equal to 5 mm, the computed value of 379 pC is smaller than the experimental peak value of 800 pC, and is not much different from the experimental most probable value of 500 pC.

Fig. 7.1 shows a comparison of the results of theoretical computations with the experimental results published in the literature [21], for the apparent charge versus applied voltage, with parameters as indicated.

It is seen from Fig. 7.1 that the computed values agree reasonably with the experimental ones. The computed values of q, which correspond

Table 7.1

Comparison of Results of Computations with
Experimental Results Published in Literature [20];
ϵ_r = 2.3, t = 0.18 mm, h = 25 mm, l = 3,
E_{av} = 6.4556 kV/mm, assumed k = 0.3

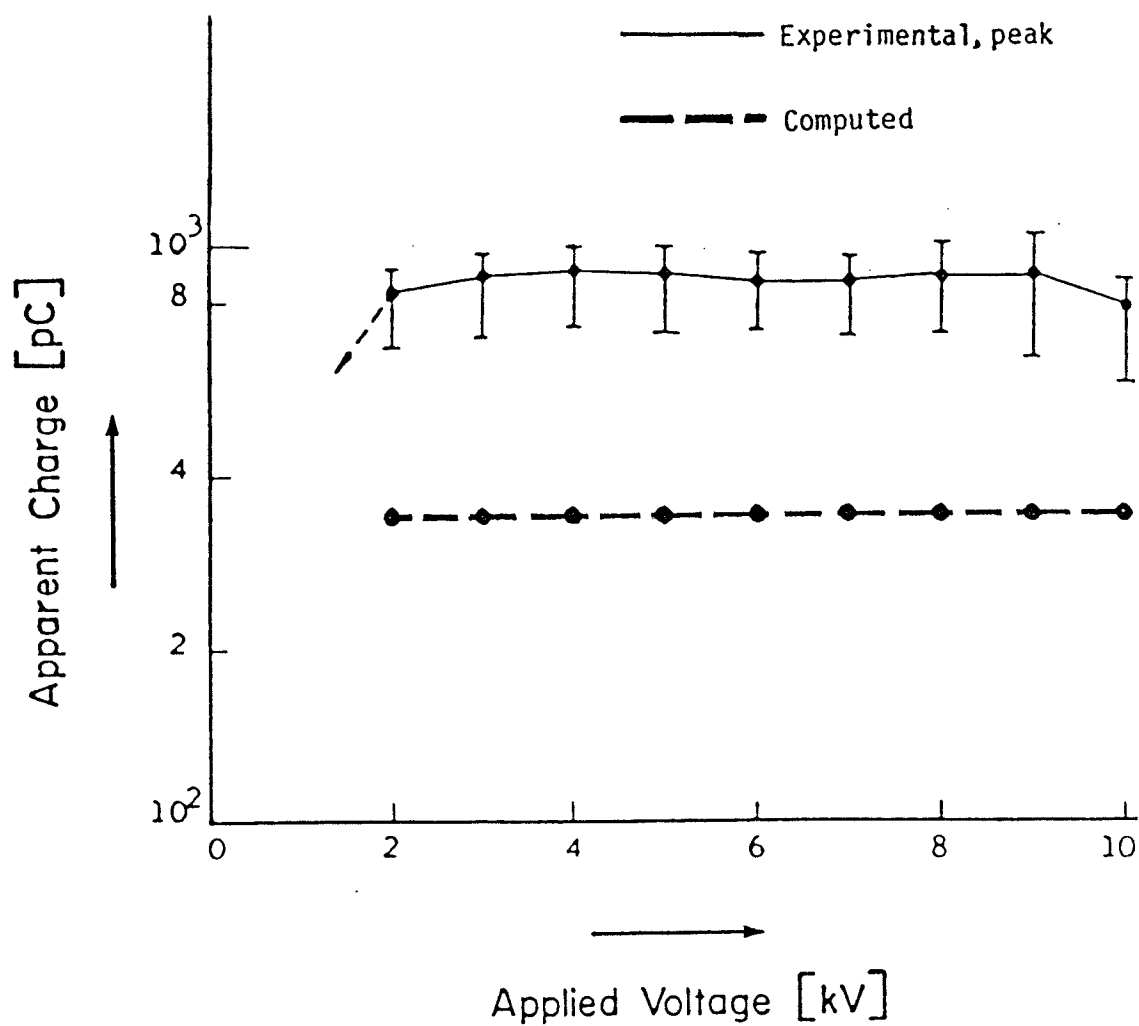| d	q [pC]		
[mm]	Experimental, from Literature		Computed
	Most Probable	Peak	
2	30	90	62
3.2	180	400	158
5	500	800	379

Fig. 7.1: Comparison of results of computations with experimental
results published in literature [21], for apparent charge versus
applied voltage:
ϵ_r = 2.3, t = 0.2mm; d = 5 mm; h = 25 mm; 1 = 3; f = 50 Hz;
assumed k = 0.3.

to average values, are always smaller than the experimental peak values of q. The computed values of q are independent of the applied voltage, while the experimental peak values of q show very small variation with the applied voltage.

Fig. 7.2 shows a comparison of the results of theoretical computations with the results published in the literature [21], for the apparent charge, with parameters as indicated. The results published are the experimental ones as well as the theoretically calculated ones. Relevant comparisons can only be carried out for the case when the degradation of the insulation has not yet occurred, i.e., just after the voltage application to the insulation. Therefore, both the theoretically computed value and the published theoretically calculated value are shown for the time after the voltage application from 0 to 6 min.

It is seen from Fig. 7.2 that the computed value of q agrees reasonably with the published experimental peak values of q. The computed value of q, which corresponds to the average value, is always smaller than the experimental peak value. On the other hand, from Fig. 7.2, the published theoretically calculated value of q, which corresponds to the average value, does not agree with the experimental peak value published in the same work [21]. The calculated value is for some samples larger than the experimental peak value.

Fig. 7.3 shows a comparison of the results of theoretical computations with the results published in the literature [21], for the apparent charge and the repetition rate for half-cycles, with parameters as indicated. The published results include experimental as well as theoretically obtained results. Since the published results of the

Fig. 7.2:   Comparison of results of computations with published in
literature [21] calculated and experimental results, for apparent
charge:
$\epsilon_r = 2.3$; t = 0.2mm; d = 1.5mm; h = 25mm; l = 3;
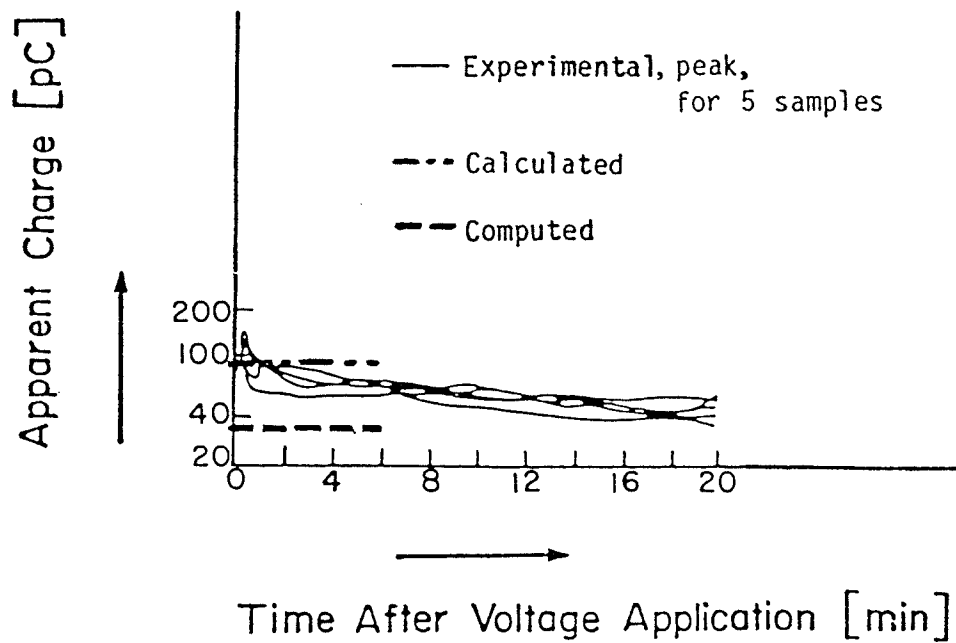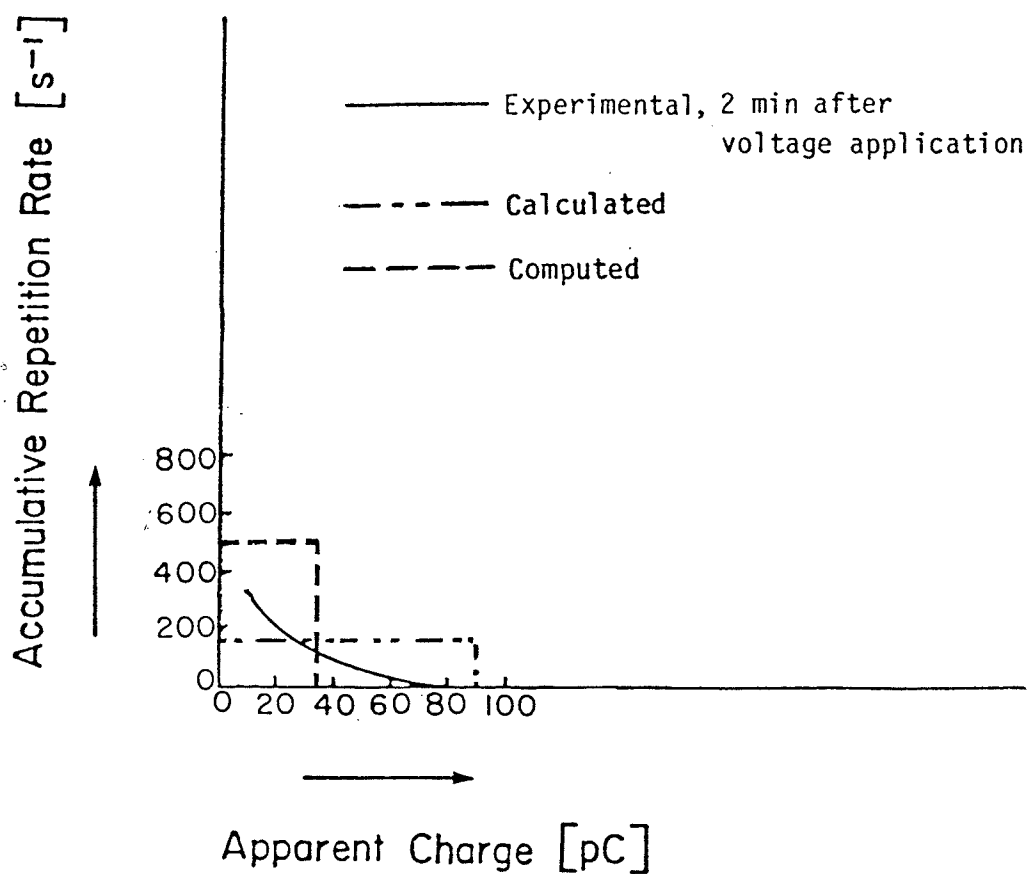E_{av} = 6.6667 kV/mm; f = 50 Hz; assumed k = 0.3.

Fig. 7.3:   Comparison of results of computations with published in
literature [21] calculated and experimental results, for apparent
charge and repetition rate for half-cycles:
ϵ_r = 2.3; t = 0.2mm; d = 1.5mm; h = 25mm; l = 3;
E_{av} = 6.6667 kV/mm; f = 50 Hz; assumed k = 0.3.

repetition rate have been expressed for half-cycles in the literature [21], the theoretical computations for the comparison, Fig. 7.3, were also performed to obtain the repetition rate for half-cycles. It may be noted that the computed repetition rate for half-cycles is equal to one half of the corresponding total repetition rate n. Therefore, the relationships which are true for the former repetition rate are also true for the latter one.

The experimental graph, Fig. 7.3, shows the accumulative distribution of discharge pulses in a cavity. The values theoretically computed in this thesis as well as those theoretically calculated in [21] form the straight lines of the accumulative distribution of discharge pulses in an ideal cylindrical cavity, Fig. 7.3.

It is seen from Fig. 7.3 that the computed distribution agrees reasonably with the published experimental one. The computed distribution, which corresponds to the average value of q, has all the discharges of q = 34 pC, which is smaller than the experimental peak value of about 80 pC, Fig. 7.3. On the other hand, from Fig. 7.3, the published theoretically calculated distribution does not agree with the experimental one published in the same work [21]. The calculated distribution, which corresponds to the average value of q, has all the discharges of q = 90.3 pC, which is larger than the experimental peak value of about 80 pC.

It may be noticed from Fig. 7.3 that the computed value of the repetition rate for half-cycles, which is equal to 500 s^{-1}, seems to agree with the published experimental one. The experimental graph ends, at the apparent charge of about 10 pC and the accumulative repetition

rate for half-cycles of about 350 s^{-1}, probably because the measurements
have not been performed for smaller thresholds of the apparent charge.
Those measurements, had they been performed, could only add an addition-
al number of discharges to the experimental value of about 350 s^{-1},
therefore making the experimental value closer to, or probably even
exceeding, the value of 500 s^{-1} computed in this thesis. On the other
hand, from Fig. 7.3, the published theoretically calculated value of the
repetition rate for half-cycles, which is equal to 164 s^{-1}, does not
agree with the published experimental one. The experimental value,
which has been reported as equal to about 350 s^{-1}, would differ even
more from the calculated value of 164 s^{-1}, if the above mentioned
measurements had been performed.

Fig. 7.4 shows a comparison of the results of theoretical computa-
tions with the experimental results published in recent literature [22],
for phase distribution of discharge pulses, with parameters as indi-
cated. The experimental distribution is obtained for the case when the
degradation of the insulation has not yet occurred, i.e. just after the
voltage application to the insulation.

It is seen from Fig. 7.4 that the computed phase distribution is
similar to the experimental one. Most of the experimental discharge
pulses occur in the same phase windows, each of 15° el width, in which
the theoretical pulses, from computations, occur.

7.3   CONCLUSIONS

The results of computations have been compared with experimental
results, published in recent literature [20-22], obtained using labora-

Phase Distribution of Discharge Pulses $[s^{-1}]$
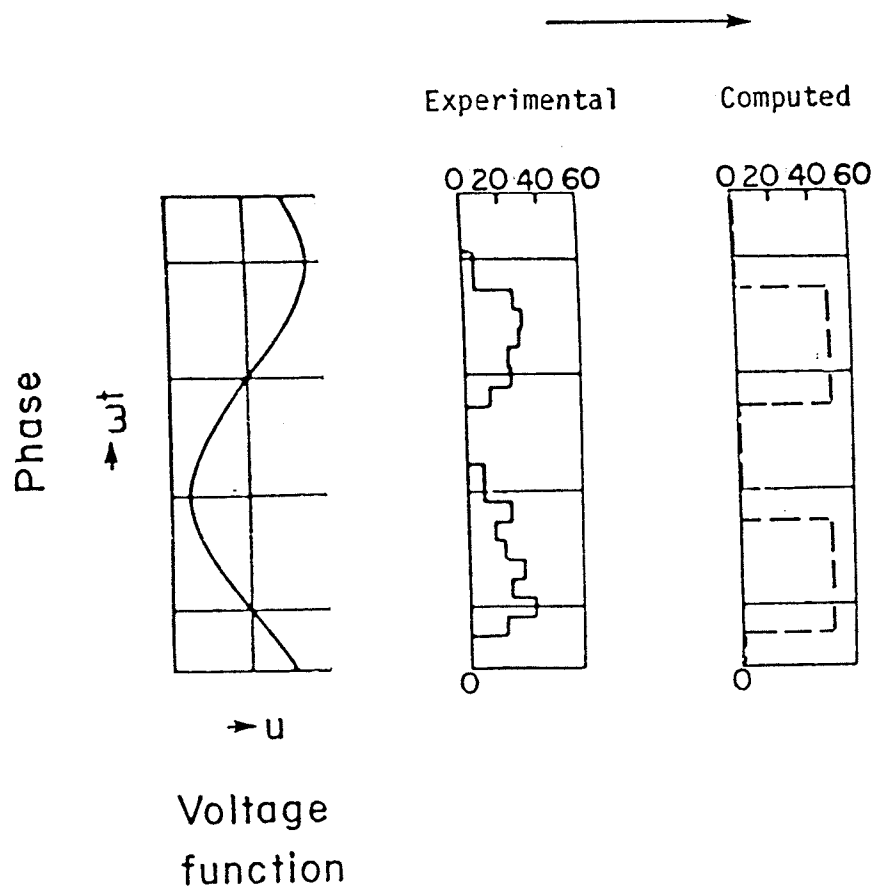
Fig. 7.4: Comparison of results of computations with experimental results published in literature [22], for phase distribution of discharge pulses:
ϵ_r = 2.3; t = 0.235mm; d = 1mm; h = 25mm; l = 3;
E_{av} = 6.3830 kV/mm; f = 50 Hz; assumed k = 0.5.

tory model insulation arrangements identical to the one considered in this thesis. The procedure of computations employing the new and more accurate pattern of recurrence of discharges has been used.

Reasonable agreement has been found between experimental and computed values of the apparent charge q, the repetition rate n and the distribution of discharge pulses [20-22]. Several examples of this agreement have been shown.

CHAPTER VIII

ADVANTAGES ASSOCIATED WITH USE
OF THE NEW DEFINITION OF DISCHARGE INTENSITY

8.1   INTRODUCTION

In this chapter the advantages associated with the use of the new definition of discharge intensity, $n_u/(n_u + n_1)$, as an indicator, over the use of the indicators q, n, n_u and n_1 are explained.

It is shown that the apparent charge q, the repetition rate n, and its components n_u and n_1, are all influenced strongly by the value of the discharge coefficient k, whereas the new proposed indicator $n_u/(n_u + n_1)$ is virtually free of this undesirable dependence. The undesirability of dependence of an indicator of discharge intensity on k is explained.

8.2   RESULTS OF COMPUTATIONS EXAMINING DEPENDENCE
OF DISCHARGE INTENSITY ON DISCHARGE COEFFICIENT

Fig. 8.1 shows the computed dependence of the quantities n, n_u, n_1, $n_u/(n_u + n_1)$ and q on the discharge coefficient k, $k = (V_i - V_e)/V_i$. The values of k considered are the typical values reported in the literature [1,2,4,7,8,13,14,22]. They have been dealt with in the second paragraph of Section 7.2. The parameters of the insulation arrangement and the voltage range considered are identical to those considered in recent experimental study [22]. The procedure of computations employing the new and more accurate pattern of recurrence of discharges was used.

It is seen from Fig. 8.1 that the apparent charge q, the repetition rate n and the indicators n_u and n_1 are all influenced strongly by the
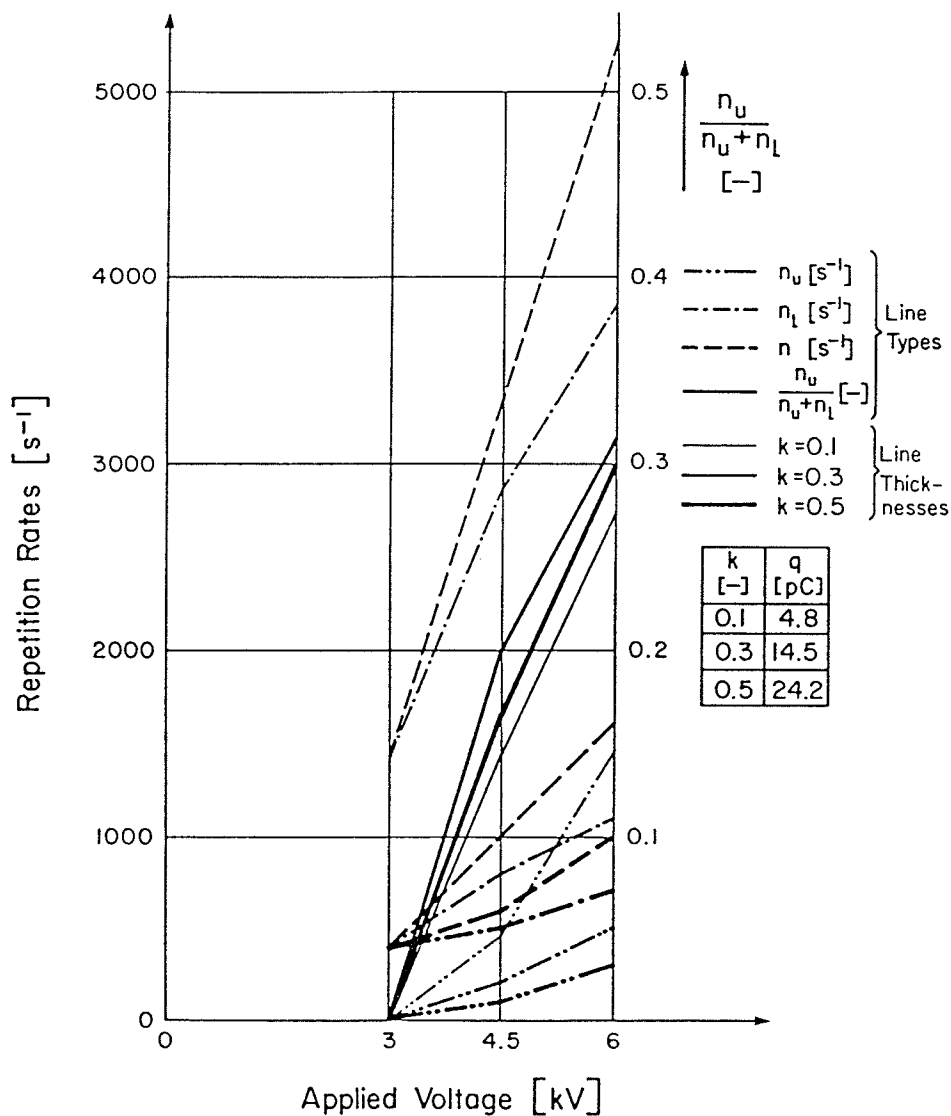
Fig. 8.1:   Results of computations of discharge intensity for:
ϵ_r = 2.3; t = 0.235 mm; l = 3; d = 1 mm; h = 25 mm; f = 50 Hz.

As indicated in the legend there are four line types i.e. solid, broken, etc., corresponding to four different functions i.e. n_u, n_l, n, $n_u/(n_u + n_l)$ and three line thicknesses corresponding to three different values of k. In total, there are 12 graphs which represent all possible combinations of line types and thicknesses. For example, the graph drawn in solid line with maximum thickness shows the variation of $n_u/(n_u + n_l)$ versus applied voltage for the case when k = 0.5.

value of the coefficient k. However, the values of $n_u/(n_u + n_l)$ are virtually free of this undesirable dependence. It may be noted that q is independent of voltage and hence its values have been tabulated. As the value of the coefficient k varies from 0.1 to 0.5, the apparent charge q increases about five times from 4.8 to 24.2 pC.

A decrease in the coefficient k implies more discharges of smaller magnitude whereas an increase implies fewer discharges but of larger magnitude. It is possible that the value of k may change during the course of an experiment. Moreover the value of k may differ from one insulating material to another, and often its exact value is not known. It is doubtful that the risk of insulation failure will change significantly with change in the value of k only. Since the new indicator, $n_u/(n_u + n_l)$, has insignificant dependence on k, it is considered to be free from a disadvantage associated with other indicators such as q, n, n_u and n_l.

It may be noted that the measurement of the total discharge repetition rate n is not considered as an insignificant indicator. Since the value of n must be used in the calculation of the discharge energy loss, which is directly related to the degradation rate of the insulation subjected to discharges, the indicator n constitutes one of the more useful measures of the internal partial discharge effect. However, due to the reason given in the last sentence of the preceding paragraph the new indicator, $n_u/(n_u + n_l)$, is considered to be free from a disadvantage associated with the indicator n. It may also be noted that since $n = n_u + n_l$, then the application of the new indicator, $n_u/(n_u + n_l)$, when obtained by the measurement of n_u and n_l, involves the information

needed to know the value of n as the sum of n_u and n_l.

8.3   CONCLUSIONS

The advantages associated with the use of the new definition of discharge intensity, $n_u/(n_u + n_l)$, as an indicator, over the use of the indicators q, n, n_u and n_l have been explained.

It has been shown that the apparent charge q, the repetition rate n, and its components n_u and n_l, are all influenced strongly by the value of the discharge coefficient k, whereas the new proposed indicator $n_u/(n_u + n_l)$ is virtually free of this undesirable dependence.   The undesirability of dependence of an indicator of discharge intensity on k has been explained.

CHAPTER IX

CONCLUSIONS

9.1   GENERAL CONCLUSIONS

The main objective of this thesis has been to propose a new defini-
tion of internal partial discharge intensity which, as an indicator, is
relatively free from disadvantages associated with presently existing
indicators.

Based on the results of analytical and digital studies, and also a
comparison with experimental studies published in recent literature, the
following conclusions are drawn:

1)   The presently used indicators of discharge intensity, the
apparent charge q and the repetition rate n, depend strongly on the
value of the discharge coefficient k.   The new proposed indicator is
virtually free of this undesirable dependence.

2)   The results of computations indicate that for "similar condi-
tions" existing at the discharge site i.e. similar values of the average
discharge current transferred across the discharging cavity, I_c, signi-
ficant differences are obtained in the theoretical values of a presently
used indicator of discharge intensity, the apparent charge q.   The
theoretical values of the new proposed indicator, $n_u/(n_u + n_l)$, do not
differ significantly.

3)   The apparent charge q often underestimates the risk of insula-
tion failure, whereas the new proposed indicator does not do so.

4)   The values of q and n computed by the procedures adopted in
the thesis agree reasonably with experimental results published in

recent literature for identical insulation arrangements.

5)   The results of computations show that for "similar conditions" existing at the discharge site, significant differences are obtained in the theoretical values of less frequently used indicators of discharge intensity, the average discharge current I and the quadratic rate D, whereas, as pointed out above in the conclusion 2), the values of the new proposed indicator do not differ significantly.

6)   The results of computations reveal that for "similar conditions" existing at the discharge site, the values of a less frequently used indicator of discharge intensity, the discharge power P, do not differ significantly. However, the new proposed indicator is easier to measure than the less frequently used indicator P.

7)   A comparison of the results of computations employing two different patterns of recurrence of discharges, the new and more accurate pattern, and the commonly used pattern, indicates that when the repetition rate or an indicator derived from it I, D or P is applied, the new pattern leads, in general, to a more conservative assessment of the risk of insulation failure than the commonly used pattern does. It may be noted however that the indicators do not depend strongly on the choice of a pattern of recurrence.

9.2   RELEVANT OBSERVATIONS

For the insulation arrangements studied, the following observations are made:

1)   The values of the discharge power of unlike discharges in negative half-cycle, P_{un}, Table 6.2, are negative which means that the energy

flow associated with unlike discharges in the negative half-cycle is directed from the insulation to the voltage source. Also, the energy flow associated with unlike discharges in the positive half-cycle is directed from the insulation to the voltage source.

2)   The above observation 1) can be explained by the fact that the electric current exchanged between the voltage source and the insulation due to a discharge is the result of the voltage drop ΔV_a across the insulation. This current flow occurs during the recharging of the insulation from the voltage source when the compensating voltage gain ΔV_{ar} is produced. For like discharges the voltage drop ΔV_a is positive, therefore the current flows from the source to the insulation and recharging it, produces the positive voltage gain ΔV_{ar}. However, from Fig. 3.3, for unlike discharges the voltage drop ΔV_a is negative, therefore the current flows from the insulation to the source and produces the negative voltage gain ΔV_{ar}. Hence, the energy flow associated with unlike discharges, in the positive as well as in the negative half-cycles, is directed from the insulation to the voltage source.

3)   The difference between the two patterns of recurrence of discharges, the new and more accurate pattern, and the commonly used pattern, diminishes as the inequalities $C_a \gg C_b$ and $C_c \gg C_b$ get more pronounced. The above inequalities are true for most practical insulation systems but may not be true for many laboratory model insulation systems.

4)   The above observation 3) can be explained by the fact that, from Fig. A.1 (in the Appendix) or Fig. 3.2, the difference between the two patterns diminishes when the voltage drop ΔV_{cr} becomes smaller in com-

parison to the voltage drop ΔV_c. It follows from formula (3.1) that as the inequality $C_c \gg C_b$ is more pronounced, the voltage drop ΔV_{cr} becomes smaller in comparison to the voltage drop ΔV_a. Next, it follows from formula (2.8) that as the inequality $C_a \gg C_b$ is more pronounced, the voltage drop ΔV_a becomes smaller in comparison to the voltage drop ΔV_c. Therefore, ΔV_{cr} becomes smaller in comparison to ΔV_c, as the inequalities $C_a \gg C_b$ and $C_c \gg C_b$ get more pronounced.

9.3   MAJOR CONTRIBUTIONS

1)   A novel approach to define internal partial discharge intensity, as the ratio $n_u/(n_u + n_l)$, based on an introduction of repetition rates of unlike discharges n_u, and of like discharges n_l, has been suggested and examined.

2)   Based on an identification of four groups of discharges the new indicators of discharge intensity have been introduced and examined; further combining of these groups in two groups has led to the introduction of the indicators n_u and n_l.

3)   A novel approach of examining the indicators for an undesirability of their dependence on the value of the discharge coefficient k, has been suggested and carried out.

4)   Detailed studies have been conducted to examine the advantages of employing the new proposed indicator, $n_u/(n_u + n_l)$, in place of other new proposed as well as traditionally used indicators.

5)   A new concept of checking that "similar conditions," which were introduced in earlier work, do exist in a set of insulation arrangements, based on an introduction of the new, nonmeasurable

quantity I_c, has been suggested and used.

6) Two patterns of recurrence of discharges, the new and the commonly used, have been compared for the difference of their assessment of the risk of insulation failure.

7) Two new procedures of digital computations of theoretical values of the new and presently used indicators for a set of insulation arrangements, one applying the introduced in earlier work, new and more accurate pattern of recurrence of discharges, and the other applying the commonly used pattern, have been developed and used.

8) A comparison of theoretical values of two most commonly used indicators of discharge intensity with published experimental results has been carried out.

9.4   SUGGESTIONS FOR FURTHER STUDIES

1) Investigating experimentally the effect of the value of the new indicator, $n_u/(n_u + n_l)$, on the lifetime of an insulation exposed to internal partial discharges, for various insulation arrangements and insulation materials.

2) Studying experimentally the possibility of establishing the "safe" values of the new indicator for various types of insulation and service conditions.

3) Investigating experimentally the "mirror image" relation between two groups of discharges in a pair of like discharges - groups (ln) and (lp), as well as in a pair of unlike discharges - groups (un) and (up).

REFERENCES

[1] J. H. Mason, "Discharges," IEEE Trans. Electr. Insul., Vol. EI-13, No. 4, August 1978, pp. 211-238.

[2] J. Bania, "Analysis of Energy Balance Associated with Internal Discharges in a Dielectric," Master's Thesis, Politechnika Lodzka, Lodz 1974, Poland. In Polish.

[3] J. P. C. McMath, "Partial Discharges in Insulation Effects and Test Methods," University of Manitoba, Winnipeg.

[4] H. C. Hall and R. M. Russek, "Discharge Inception and Extinction in Dielectric Voids," Proc. IEE, pt. II, 1954, pp. 47-55.

[5] F. H. Kreuger, "Discharge Detection in High Voltage Equipment," Heywood Book, London 1964.

[6] E. Husain and R. S. Nema, "Analysis of Paschen Curves for Air, N_2 and SF_6 Using the Townsend Breakdown Equation," IEEE Trans. Electr. Insul., Vol. EI-17, No. 4, August 1982, pp. 350-353.

[7] Z. Szczepanski and J. Bania, "Evaluation of Length of Life of a Dielectric by Erosive Action of Partial Discharges," Arch. Elektrotech., Vol. 27, No. 2, Warszawa 1978, Poland, pp. 325-334. In Polish.

[8] J. Bania, "Evaluation of Apparent Charge as an Intensity Indicator of Internal Discharges in a Dielectric," Zeszyty Naukowe Politechniki Lodzkiej Elektryka, No. 66, Lodz 1979, Poland, pp. 7-19. In Polish.

[9] N. B. Timpe and S. V. Heyer, "Laboratory and Field Partial-Discharge Studies by a Utility," IEEE Trans. Electr. Insul., Vol. EI-12, No. 2, April 1977, pp. 159-164.

[10] B. Salvage, "Electric Stresses in Gaseous Cavities in Solid Dielectrics," Proc. IEE, Vol. III, No. 6, June 1964, pp. 1162-1172.

[11] D. Kind and D. Konig, "AC Breakdown of Epoxy Resins by Partial Discharges in Voids," IEEE Trans. Electr. Insul., Vol. EI-3, No. 2, May 1968, pp. 40-46.

[12] E. Kuffel and M. Abdullah, "High-voltage Engineering," Book, Pergamon Press Ltd., Oxford 1970.

[13] Z. Szczepanski, "Partial Discharges in Electrical Equipment Insulation," Book, WNT, Warszawa 1973, Poland. In Polish.

[14] R. R. Opoku, E. G. Robles and J. H. Mason, "Degradation and Break-down of Polypropylene Film by Internal Discharges," Conference on Dielectric Materials, Measurements and Applications, Cambridge 1975, pp. 323-326.

[15] A. Kelen, "Critical Examination of the Dissipation Factor Tip-Up as a Measure of Partial Discharge Intensity," IEEE Trans. Electr. Insul., Vol. EI-13, No. 1, February 1978, pp. 14-23.

[16] International Electrotechnical Commission, IEC Recommendation, Publication 270, "Partial Discharge Measurements," Geneva 1968, Switzerland.

[17] An American National Standard ANSI C68.3-1976/IEEE Std 454-1973, "IEEE Recommended Practice for the Detection and Measurement of Partial Discharges (Corona) During Dielectric Tests."

[18] American Society for Testing and Materials D 1868-81, "Standard Method for Detection and Measurement of Partial Discharge (Corona) Pulses in Evaluation of Insulation Systems," Annual Book of ASTM Standards, Part 39, 1982, pp. 514-525.

[19] W. T. Starr in "Engineering Dielectrics," Vol. I, "Corona Inter-pretation and Measurement," R. Bartnikas and E. J. McMahon, Editors, Publ. STP 669, ASTM Press, Philadelphia, 1979.

[20] R. Miller and I. A. Black, "Partial Discharge Measurements Over the Frequency Ranges 0.1 Hz to 50 Hz," IEEE Trans. Electr. Insul., Vol. EI-12, No. 3, June 1977, pp. 224-233.

[21] T. Tanaka and Y. Ikeda, "Internal Discharges in Polyethylene with an Artificial Cavity," IEEE Trans. PAS-90, 1971, pp. 2692-2702.

[22] J. Griac, "The Effect of Additives on Extinction of Discharges in Voids in Polyethylene Insulation," I.H.V.S. Zurich 1975, pp. 576-581.

[23] M. Kurtz and G. C. Stone, "In-service Partial Discharge Testing of Generator Insulation," IEEE Trans. Electr. Insul., Vol. EI-14, No. 2, April 1979, pp. 94-100.

[24] A. S. Ahmed and A. A. Zaky, "Calibration of Partial Discharge Detectors for Pulse-height Distribution Analysis," IEEE Trans. Electr. Insul., Vol. EI-14, No. 5, October 1979, pp. 281-284.

[25] J. Golinski, J. H. Calderwood, S. Zoledziowski and A. Sierota, "Partial Discharges in a Cylindrical Void with a Metal Rod Elect-rode," IEEE Trans. Electr. Insul., Vol. EI-17, No. 6, December 1982, pp. 560-569.

[26] E. Kuffel and W. S. Zaengl, "High-voltage Engineering," Book, Pergamon Press, 1984.

APPENDIX

TYPICAL ENERGY BALANCE CALCULATION

A typical energy balance calculation is presented for the case of discharges shown in Fig. A.1, in order to illustrate the effect of neglecting, in the commonly used pattern or recurrence, insulation recharging from the voltage source.

The three energy states of Table 3.1, which were introduced in [2], allow one to calculate the energy dissipated due to a discharge as

$$\Delta E_{diss} = E_c'' + E_b'' + E_a'' - E_c' - E_b' - E_a' \tag{A.1}$$

and the energy supplied due to recharging from the voltage source as

$$\Delta E_{supp} = E_c''' + E_b''' + E_a''' - E_c'' - E_b'' - E_a'' \tag{A.2}$$

The total energy change due to a discharge and subsequent recharging is

$$\Delta E = \Delta E_{diss} + \Delta E_{supp}$$
$$= E_c''' + E_b''' + E_a''' - E_c' - E_b' - E_a' \tag{A.3}$$

The values of ΔE_{diss}, ΔE_{supp} and ΔE will be calculated from (A.1), (A.2) and (A.3) respectively, for individual discharges applying the new pattern of recurrence of discharges.

With the application of the pattern of recurrence commonly used in literature the energy dissipated due to a discharge is calculated from

$$\Delta E_{diss}* = - (C_c + \frac{C_b C_a}{C_b + C_a}) \; \Delta V_c \; (V_i - \frac{1}{2} \Delta V_c) \tag{A.4}$$

and the energy supplied due to recharging from the voltage source is calculated from

$$\Delta E_{supp}* = (C_a + \frac{C_c C_b}{C_c + C_b}) \; \Delta V_a \; (V_a - \frac{1}{2} \Delta V_a) \tag{A.5}$$
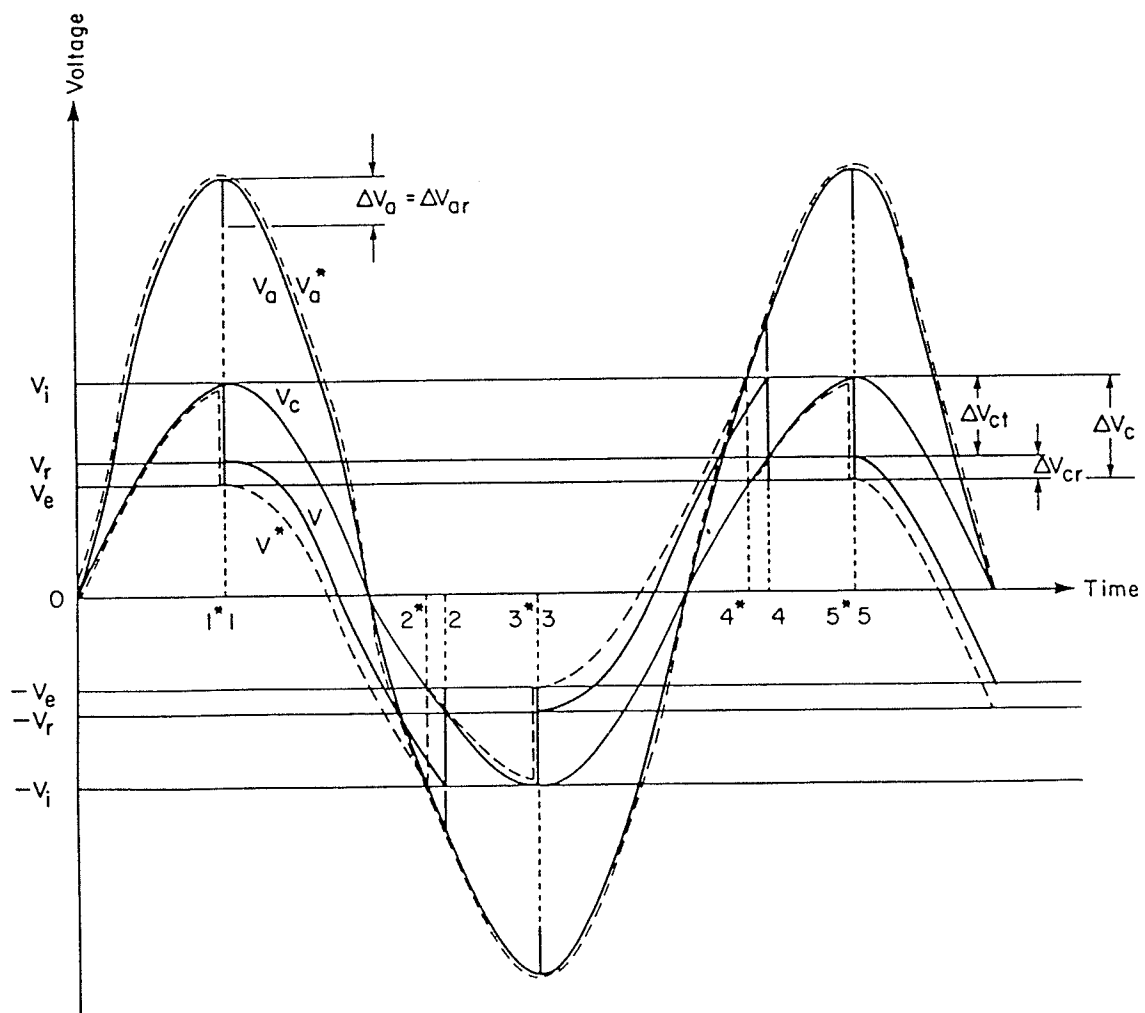
Fig. A.1: Case of discharges used to conduct typical energy balance: V, V_a - new pattern; V^*, V_a^* - commonly used pattern; numbers 1, 2, 3, 4, 5 - indicate consecutive discharges according to new pattern; numbers 1*, 2*, 3*, 4*, 5* - indicate consecutive discharges according to commonly used pattern.

The total energy change due to a discharge and subsequent recharging is calculated from

$$\Delta E_* = \Delta E_{diss*} + \Delta E_{supp*} \qquad (A.6)$$

The values of $\Delta E_{diss}*$, $\Delta E_{supp}*$ and $\Delta E*$ will be calculated from (A.4), (A.5) and (A.6) respectively, for individual discharges applying the pattern of recurrence commonly used in literature.

The following values were assumed; the capacitances in capacitance units, $C_c = 1$, $C_b = 1$, and $C_a = 1$; the inception voltage in voltage units, $V_i = 8$; the discharge coefficient k which is dimensionless, $k = 1/2$. Let us also assume that the voltage $\hat{V}_c = V_i$, therefore $\hat{V}_c = 8$, in voltage units. This is the case of discharges shown in Fig. A.1. It can be obtained that the voltage drops or gains in voltage units are, $\Delta V_c = 4$, $\Delta V_a = \Delta V_{ar} = 2$, $\Delta V_b = 2$, $\Delta V_{cr} = 1$, $\Delta V_{br} = 1$, $\Delta V_{ct} = 3$, $\Delta V_{bt} = 3$, and that the voltage $\hat{V}_a = 16$, in voltage units.

We first apply the new pattern of recurrence and the energy states of Table 3.1 [2]. It can be obtained that, in energy units (where energy unit is the product of capacitance unit and the squared voltage unit) for discharge 4:

$$E_{c4}' = 32, \qquad E_{c4}'' = 8, \qquad E_{c4}''' = 25/2,$$
$$E_{b4}' = 2, \qquad E_{b4}'' = 8, \qquad E_{b4}''' = 25/2,$$
$$E_{a4}' = 50, \qquad E_{a4}'' = 32, \qquad E_{a4}''' = 50,$$

and for discharge 5:

$$E_{c5}' = 32, \qquad E_{c5}'' = 8, \qquad E_{c5}''' = 25/2,$$
$$E_{b5}' = 32, \qquad E_{b5}'' = 50, \qquad E_{b5}''' = 121/2,$$
$$E_{a5}' = 128, \qquad E_{a5}'' = 98, \qquad E_{a5}''' = 128.$$

The energy changes for discharge 4 are:

$$\Delta E_{diss4} = E_{c4}'' + E_{b4}'' + E_{a4}'' - E_{c4}' - E_{b4}' - E_{a4}'$$

$$= -36$$

$$\Delta E_{supp4} = E_{c4}''' + E_{b4}''' + E_{a4}''' - E_{c4}'' - E_{b4}'' - E_{a4}''$$

$$= 27$$

$$\Delta E_4 = \Delta E_{diss4} + \Delta E_{supp4} = -36 + 27 = -9$$

Next, the energy changes for discharge 5 are:

$$\Delta E_{diss5} = E_{c5}'' + E_{b5}'' + E_{a5}'' - E_{c5}' - E_{b5}' - E_{a5}'$$

$$= -36$$

$$\Delta E_{supp5} = E_{c5}''' + E_{b5}''' + E_{a5}''' - E_{c5}'' - E_{b5}'' - E_{a5}''$$

$$= 45$$

$$\Delta E_5 = \Delta E_{diss5} + \Delta E_{supp5} = -36 + 45 = 9$$

Then,

$$\Delta E_{4\&5} = \Delta E_4 + \Delta E_5 = -9 + 9 = 0,$$

for half cycle of discharges 4 and 5.

The results of such an analysis of discharges 2 and 3 are identical to those obtained by analysis of discharges 4 and 5 respectively (all corresponding voltages are opposite so that their squares are identical).

Therefore,

$$\Delta E_{2\&3} = \Delta E_{4\&5} = 0$$

Since $\Delta E_{2\&3} + \Delta E_{4\&5} = 0 + 0 = 0$, for one cycle of discharges 2, 3, 4 and 5, the energy balance is satisfied when applying the new pattern of recurrence.

We now apply the pattern of recurrence commonly used in literature. It can be obtained that, in energy units, for discharge 4*:

$\Delta E_{diss4*} = -36$ $(= \Delta E_{diss4})$

and since $V_{a4*} = 8$ $(\neq V_{a4} = 10)$,

$\Delta E_{supp4*} = 21$ $(\neq \Delta E_{supp4} = 27)$

therefore,

$\Delta E_{4*} = \Delta E_{diss4*} + \Delta E_{supp4*} = -36 + 21 = -15$ $(\neq \Delta E_4 = -9)$

Next, it can be obtained that for discharge 5*:

$\Delta E_{diss5*} = -36$ $(= \Delta E_{diss5})$

and since $V_{a5*} = 16$ $(= V_{a5})$,

$\Delta E_{supp5*} = 45$ $(= \Delta E_{supp5})$

therefore,

$\Delta E_{5*} = \Delta E_{diss5*} + \Delta E_{supp5*} = -36 + 45 = 9$ $(= \Delta E_5)$

Then,

$\Delta E_{4*\&5*} = \Delta E_{4*} + \Delta E_{5*} = -15 + 9 = -6$ $(\neq \Delta E_{4\&5} = 0)$,

for half cycle of discharges 4* and 5*.

The results of such an analysis of discharges 2* and 3* are identical to those obtained by analysis of discharges 4* and 5* respectively (all corresponding voltages or voltage drops are opposite so that corresponding energy changes are identical).

Therefore,

$\Delta E_{2*\&3*} = \Delta E_{4*\&5*} = -6$

Since $\Delta E_{2*\&3*} + \Delta E_{4*\&5*} = -6 + (-6) = -12 \neq 0$, for one cycle of discharges 2*, 3*, 4* and 5*, the energy balance is not satisfied when applying the pattern of recurrence commonly used in literature.